

**ROLE OF RESIDUES ON THE PROXIMAL SIDE OF THE HEME IN
CATALASE HPII OF *Escherichia coli***

by

Bei Hu

A Thesis

Submitted to the

Faculty of Graduate Studies

in Partial Fulfillment of the Requirements

for the Degree of Master of Science

Department of Microbiology

University of Manitoba

Winnipeg, Manitoba

© December 1999



**National Library
of Canada**

**Acquisitions and
Bibliographic Services**

**395 Wellington Street
Ottawa ON K1A 0N4
Canada**

**Bibliothèque nationale
du Canada**

**Acquisitions et
services bibliographiques**

**395, rue Wellington
Ottawa ON K1A 0N4
Canada**

Your file Votre référence

Our file Notre référence

The author has granted a non-exclusive licence allowing the National Library of Canada to reproduce, loan, distribute or sell copies of this thesis in microform, paper or electronic formats.

The author retains ownership of the copyright in this thesis. Neither the thesis nor substantial extracts from it may be printed or otherwise reproduced without the author's permission.

L'auteur a accordé une licence non exclusive permettant à la Bibliothèque nationale du Canada de reproduire, prêter, distribuer ou vendre des copies de cette thèse sous la forme de microfiche/film, de reproduction sur papier ou sur format électronique.

L'auteur conserve la propriété du droit d'auteur qui protège cette thèse. Ni la thèse ni des extraits substantiels de celle-ci ne doivent être imprimés ou autrement reproduits sans son autorisation.

0-612-51756-X

Canada

**THE UNIVERSITY OF MANITOBA
FACULTY OF GRADUATE STUDIES

COPYRIGHT PERMISSION PAGE**

**Role of Residues on the Proximal Side of the Heme in
Catalase HPII of *Escherichia coli***

BY

Bei Hu

**A Thesis/Practicum submitted to the Faculty of Graduate Studies of The University
of Manitoba in partial fulfillment of the requirements of the degree
of
Master of Science**

BEI HU ©1999

Permission has been granted to the Library of The University of Manitoba to lend or sell copies of this thesis/practicum, to the National Library of Canada to microfilm this thesis and to lend or sell copies of the film, and to Dissertations Abstracts International to publish an abstract of this thesis/practicum.

The author reserves other publication rights, and neither this thesis/practicum nor extensive extracts from it may be printed or otherwise reproduced without the author's written permission.

ACKNOWLEDGEMENTS

I would like to extend my thanks and gratitude to Dr. Peter Loewen for his financial support, thoughtful advice, scientific insights, patience and kind words. All of these were indispensable to the successful completion of this body of work. Several others deserve mention for their assistance. These include the other members of my graduate committee, fellow graduate students in the Department of Microbiology including but not limited to Ming Yang, Alex Hillar, Jeanna Strutinsky, Xiang Wei, Denny Wong, Lorilee Tschetter, Lesia Harahuc and Tamiko; and the entire faculty and staff of the Department of Microbiology.

Outside of the Department of Microbiology, I would especially like to thank Shanhong Hu and all those who made my short stay in Canada happier than it otherwise would have been.

Lastly, I would like thank mom and dad, sister, boyfriend and my "new parents" (Mr and Mrs Barker) for their love.

ABSTRACT

Catalase has been found in virtually all aerobic and some anaerobic organisms which degrade hydrogen peroxide to oxygen and water, and is typically a homotetramer of 65,000 Da subunits, each containing one protoheme IX prosthetic group. Hydroperoxidase II (HPH) from *Escherichia coli* has significant similarity to the typical shorter catalases from several plant, mammalian, and fungal sources, but is a tetramer of 84,000 Da subunits with four cis-hydroxy spirolactone heme d groups which are converted from protoheme in a reaction catalyzed by HPH. The additional amino acids of HPH are contained in a ~75 amino acid N-terminal segment and a ~175 amino acid C-terminal segment. The three dimensional structure of HPH exhibits several unusual structural modifications, including a covalent bond between N₅ of His392 and C₉ of Tyr415. A mechanistic explanation for the autocatalytic conversion of heme b to heme d is proposed to involve formation of this bond, with His395 and Asp197 or an anion may extract a proton from N₅ of His392, ultimately resulting in hydroxyl addition to ring III of protoheme.

Through site-directed mutagenesis the roles of the amino acids H392, H395, D197, Q419 in heme conversion were studied. H392 mutants which disable the His-Tyr bond contain only heme b as their prosthetic group, and lose specific activity, thermostability and sensitivity to the inhibitors NaCN, NaN₃, NH₂OH, CH₃ONH₂, C₂H₅ONH₂ compared to wild type HPH. Populations of D197S/H395Q and Q419A mutant HPH contain both heme b and heme d as their prosthetic group, and are less thermostable compared to wild type HPH, but

retain wild type HP11 characteristics regarding enzyme kinetics and inhibitor sensitivity. H395A, H395Q, D197A, D197S and Q419H mutants showed no significant differences when compared to wild type HP11.

It therefore appears that, while His392, His395, Asp197 and Gln419 are all involved in heme conversion, only the presence of His392 is absolutely critical for the reaction to proceed. These results support the mechanistic relationship between the proposed autocatalytic conversion of heme b to heme d mechanism proposed by Bravo *et al.* (1997a).

TABLE OF CONTENTS

	Page
ACKNOWLEDGMENTS	i
ABSTRACT	ii
TABLE OF CONTENTS	iv
LIST OF FIGURES	vi
LIST OF TABLES	viii
LIST OF ABBREVIATIONS	ix
1. HISTORICAL	1
• Reactive Oxygen Species	1
• Toxicity of Hydrogen Peroxide	2
• Catalase Reactions	3
• Phylogenetic relations and grouping among catalases	4
• The catalase reaction mechanism	7
• Properties of HPII	10
• Regulation of HPII synthesis	10
• Structure of typical catalase: BLC	13
• Structure of HPII	14
• Structural features of bovine liver catalase	16
• Heme binding in HPII	17
• Thesis objective	21
2. EXPERIMENTAL PROCEDURE	22
2.1. <i>Escherichia coli</i> STRAINS, PLASMIDS AND BACTERIOPHAGE	22
2.2. GROWTH MEDIA, CONDITIONS AND STORAGE CULTURE	22
2.3. SITE-DIRECTED MUTAGENESIS STRATEGY	24
2.3.A. Preparation and isolation of oligonucleotides	25
2.3.B. Uracil-containing single stranded DNA isolation	31
2.3.C. Site-directed mutagenesis	31
2.3.D. Transformation	32
2.3.E. Plasmid isolation and purification	33
2.3.F. Restriction endonuclease digestion of DNA	33
2.3.G. Agarose gel electrophoresis	33
2.3.H. Single Stranded DNA sequencing	34
2.3.J. DNA bands recovering	34

2.4. PROTEIN PURIFICATION	34
2.5. PROTEIN CHARACTERIZATION	35
2.5.A. Sodium dodecyl sulfate-polyacrylamide gel electrophoresis (SDS-PAGE)	36
2.5.B. Catalase activity assay and Protein quantification	36
2.5.C. Inhibition studies	37
2.5.D. High Performance Liquid Chromatography	37
3. RESULTS and DISCUSSION	38
Section I: Construction of mutant catalase HPiIs	38
Section II: Purification of mutant catalase HPiIs	38
Section III: Characterization of mutant catalase HPiIs	44
● Effect of Temperature on Mutant Catalase HPiI Expression	44
● Spectral Properties of Mutant Catalase HPiIs	46
● Specific Activity and Steady-state Kinetic Properties of Mutant Catalase HPiIs	54
● Effect of High Temperature on Mutant Catalase HPiI Activities	56
● Effect of Cyanide and Azide on Mutant Catalase HPiI Activities	57
● Effect of NH_2OH , CH_3ONH_2 , $\text{C}_2\text{H}_5\text{ONH}_2$ on Mutant Catalase HPiIs	64
Summary	75
4. REFERENCES	77

LIST OF FIGURES

Figure		Page
1.1.	A proposed mechanism coupling the formation of the His-Tyr bond to the oxidation of ring III of the heme in HP11 of <i>E. coli</i> . (Bravo, J. et al., 1997)	20
2.1	The DNA sequence of the insert of <i>katE</i> gene within pAMkatE72. The sequences of the mutagenic primers, sequencing primers and the restriction enzymes used in cloning are also shown. (data modified from von Ossowski et al., 1991)	26
3.1.1.	Figure of residues in region particularly the ones changed.	39
3.1.2.	Autoradiograms of sequencing gels revealing base changes in the codon sites for Asp197, His392, His395, Gln419 in HP11 catalase.	40
3.2.1.	SDS-polyacrylamide gel electrophoresis analysis of various mutants of HP11 following purification. Samples of approximately 10 μ g were electrophoresed on an 8% gel and stained with Coomassie Brilliant Blue.	43
3.3.1.	Elution profile from C18 reverse phase HPLC chromatography of heme extracted from various HP11 mutants. The letter 'b' and 'd' denote the locations of heme b and heme d respectively.	48
3.3.2.	Absorption spectra of wild type HP11 and various mutants. The left axis is for the range from 350-475 nm while the right axis is for the range from 475 to 750 nm.	51
3.3.3.	Comparison of the effect of hydrogen peroxide concentrations on the initial velocities (V_i) of wild type HP11 and various mutants.	59
3.3.4.	Determination of the activity of mutant and wild type HP11 catalases during incubation at 65°C. Each of the enzymes was incubated at 65°C in 50 mM potassium phosphate buffer (pH 7.0), and aliquots were removed at various times and assayed. Data are expressed as a percentage of original activity.	63

- 3.3.5. Comparison of the effects of sodium azide on mutant and wild type HP11 catalase activities. 65**
- 3.3.6. Comparison of the effects of sodium cyanide on mutant and wild type HP11 catalase activities. 66**
- 3.3.7. Absorption spectra of mutant and wild type HP11 catalases in the presence and absence (_____) of NaCN and NaN₃. Each enzyme was incubated with 0.5mM NaCN(——) and 1 mM NaN₃ (.....) at room temperature for 15 min prior to spectral analysis. The left axis is for the range from 350 to 475nm while the right axis is for the range from 475 to 750 nm. 67**
- 3.3.8 Comparison of the effects of various hydroxylamine derivatives on mutant D197A, D197S, D197S/H395Q and wild type HP11 catalases activities. 70**
- 3.3.9. Comparison of the effects of various hydroxylamine derivatives on mutant H392A, H392Q and wild type HP11 catalases activities. 71**
- 3.3.10. Comparison of the effects of various hydroxylamine derivatives on mutant H395A, H395Q and wild type HP11 catalases activities 72**
- 3.3.11 Comparison of the effects of various hydroxylamine derivatives on mutant Q419A, Q419H and wild type HP11 catalases activities. 73**

LIST OF TABLES

Table		Page
2.1.	List of <i>E. coli</i> strains, plasmids and bacteriophage used in project.	23
2.2.	Sequences of the oligonucleotides used for site-directed mutagenesis of <i>katE</i>	30
3.3.1.	Comparison of the effect of the culture growth temperature on the production of the wild type and mutant catalase HPiIs. Proteins are extracted from cultures inoculated overnight at 28°C and 37°C.	45
3.3.2.	Comparison of the prosthetic groups of wild type and mutant variants of HPiI	47
3.3.3.	Specific activities and kinetic parameters of the mutant and wild type of HPiI catalases	58
3.3.4.	Determination of the 50% inhibitory concentrations of nine mutant HPiI catalases compared with wild type HPiI enzyme.	74

LIST OF ABBREVIATIONS

A	Absorbance
Amp ^r	Ampicillin resistant
BLC	Bovine liver catalase
bp	Base pair(s)
CCA	convex constrain algorithm
Da	Dalton
DEAE	Diethylaminoethyl
DMSO	Dimethylsulfoxide
DNA	Deoxyribonucleic acid
DTT	Dithiothreitol
EDTA	Ethylenediaminetetraacetic acid
HP I	Hydroperoxidase I
HP II	Hydroperoxidase II
HPLC	High performance liquid chromatography
K _{cat}	Turnover number
kDa	KiloDalton
K _m	Michaelis-Menten constant
LB	Luria-Bertani medium
2-ME	2-Mercaptoethanol
MW	Molecular weight
NADPH	Nicotinamide adeninedinucleotide phosphate
PAGE	Polyacrylamide gel electrophoresis
PVC	<i>Penicillium vitale</i> catalase
SDS	Sodium dodecyl sulfate
V _{max}	Maximum velocity
V _i	Initial velocity
WT	Wild type
w/v	Weight per volume

1. HISTORICAL

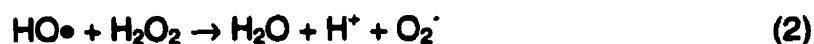
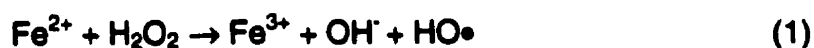
Reactive Oxygen Species

Oxygen is the most abundant element in the earth's crust with an atomic abundance of 53.8% while its atmospheric concentration amounts to 21%. Oxygen in its most stable state has two unpaired electrons in two different π^* orbitals with parallel spins. Theoretically, two electrons are required to reduce it to water. However, according to Pauli's exclusion principle, electrons in the same orbital will have antiparallel spins (Dickerson *et al.*, 1984). Oxygen's reactions with nonradicals are limited and it has been shown to be a relatively unreactive molecule which does not display an overt toxicity (Dempsey, 1991, Farr and Kogoma, 1991). However, several active oxygen species of varying reactivities can be generated as by-products of oxygen reactions in a variety of ways including: normal aerobic respiration (Halliwell and Gutteridge, 1989); enzymatic reactions including those catalyzed by D-amino acid oxidases, a number of dehydrogenases and glutathione reductase, nitric-oxide synthase (Imay and Fridovich, 1991; Farr and Kogoma, 1991; Xia *et al.*, 1998); the autoxidation of a number of compounds such as ubiquinol, catechols, thiol, flavins and ascorbate; exposure to environmental factors such as ionizing radiation and ultraviolet light; other factors including ozone, ultrasound, lithotripsy, freeze-drying, transforming growth factor β 1 in lung fibroblast cell and drugs such as paraquat; macrophages in response to bacterial invasion in the mammalian body; and from other organisms in the environment (Fridovich, 1978; Chance *et al.*, 1979; Ames, 1983; Cerutti, 1985; Cross *et al.*, 1987; Halliwell and Gutteridge,

1989). Reactive oxygen species include hydroxyl radicals (HO•), hydroperoxyl radicals (HOO•), superoxide anions (O₂⁻), singlet oxygen (¹O₂), and hydrogen peroxide (H₂O₂). These oxygen species are toxic because they can damage DNA (Brawn and Fridovich, 1981; Demple and Linn, 1982), oxidize protein (Brot *et al.*, 1981. Daviies *et al.*, 1987), membrane fatty acids (Mead, 1976; Fridovich & Porter, 1981), and have been linked to several diseases such as rheumatoid arthritis, inflammatory bowel disorders, and atherosclerosis (Farr and Kogoma, 1991). Moreover, these oxygen molecules also appear to play a part in advancing mutagenesis, tumorigenesis, and aging (Farr and Kogoma, 1991).

Toxicity of Hydrogen Peroxide

While it is known that HO• is the most toxic oxygen species, hydrogen peroxide is one of the least potent within this group (Halliwell and Gutteridge, 1986). Despite this, hydrogen peroxide is still a strong oxidant and can be detrimental to the cell through reactions such as the oxidation of thiol groups in proteins, of glutathione (Brodie and Reed, 1987) and of keto-acids (Halliwell and Gutteridge, 1990). However, hydrogen peroxide cannot damage purified DNA unless an iron or other metal ion is available (Filho *et al.*, 1984) to catalyze the Haber-Weiss reaction, in which hydrogen peroxide is converted into the highly reactive hydroxyl radical (Fenton, 1894; Haber & Weiss, 1934) as follows:(1-5):

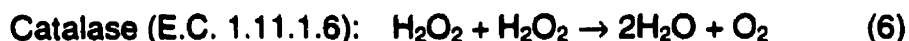




The various highly reactive intermediates can be lethal to bacterial and fungal spores (Marquis & Shin, 1994; Levitz & Diamond, 1984). The hydroxyl radical can react rapidly with most cellular components in reactions involving hydrogen abstraction. Furthermore, in the presence of excess hydrogen peroxide, several iron-containing proteins are damaged causing the release of iron that may be used for Haber-Weiss reaction (Gutteridge, 1986).

Catalase Reactions

Protective mechanism(s) to rid the cell of hydrogen peroxide must have developed early in the course of evolution once oxygen had become an important environmental component. The principle mechanism now is the catalytic activity of the hydroperoxidases, which include the catalases and peroxidases, in the following reactions(6)(7):



In the peroxidase reaction, hydrogen peroxide is converted into water using an organic or halide electron donor as substrate without the formation of oxygen. In contrast, catalase, or hydrogen peroxide — hydrogen peroxide oxidoreductase, decomposes and converts the hydrogen peroxide to water and oxygen with a very rapid turnover rate. As well as being one of the first enzymes described (Gottstein, 1893; Loew, 1901), catalases have been isolated from

virtually all aerobic cells, including animals (Desiseroth and Dounce, 1970), plants (Esaka and Asahi, 1982) and microorganisms (Herbert and Pinsent, 1948). Beef liver catalase (BLC) was also one of the first proteins to be successfully crystallized (Sumner and Dounce, 1937) and remains one of the best characterized catalases in terms of general biochemical, kinetic, and structural data. Most catalases are homotetramers with molecular weights of approximately 240 kilodaltons (kD), and a heme prosthetic group in each subunit, although a number of variations are evident. Some catalases also have a peroxidase activity and are referred to as catalase-peroxidases. They are distinctly different from the monofunctional catalases.

Phylogenetic relations and grouping among catalases

The first catalase of eukaryotic origin to be partially purified was from tobacco plant in 1901 (Loew 1901). Half a century later, catalase from *Micrococcus luteus* was the first catalase of prokaryotic origin to be purified (Herbert and Pinsent 1948). It was only after the purification of hydroperoxidase I (HPI) and hydroperoxidase II (HP II) from *Escherichia coli* in 1979, both of which differed from their eukaryotic counterparts (Claiborne and Fridovich 1979; Claiborne et al. 1979; Loewen and Switala 1986), that a significant number (approximately 100) of sequences of catalases from all sources have been reported. Alignment of 74 monofunctional catalase protein sequences, spanning bacterial, fungal, animal and plant sources, reveals a conserved core region of approximately 360 amino acids with significant sequence similarity among all

catalases. On either side of this conserved core, sequences are more divergent, although the subgroup of large-subunit catalases (more than 650 residues) retain some similarity in the extended carboxyl domain (Klotz *et al.* 1997).

An unrooted phylogenetic tree based on the core amino acid sequence of 70 catalases has been constructed by parsimony and distance methods by Klotz *et al.* (1997). Similar trees have also been derived using the full lengths of the catalase sequences (Klotz *et al.* 1997). Catalase-peroxidases, which have very dissimilar sequences from monofunctional catalases, were not included in both alignments. The core of the resulting tree contains distinct groups for plant and animal catalases, two groups of fungal catalases, and three groups of bacterial catalases. An overlap of kingdoms occurs within one branch involving fungal and bacterial group II enzymes. The other fungal branch is closely linked to the animal enzymes. Both Group I and Group II bacterial catalases occur in normally nonpathogenic bacteria, with Group I more closely related to the plant enzymes, and Group II composed of large-subunit catalases overlapping fungal group II. Group III bacterial sequences are more closely related to fungal group I and animal sequences and include enzymes mainly from pathogenic bacteria (Loewen 1997; Klotz *et al.* 1997).

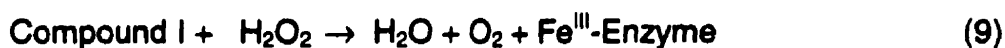
A mechanism for the evolution of catalases was proposed that combines these groups into three catalase gene families (consisting of 1. plant catalases and group I bacterial catalases; 2. large subunit bacterial and fungal enzymes; 3. fungal I, group III bacterial and animal catalases) which all arise from a common progenitor gene through two gene duplication events (Klotz *et al.* 1997).

Based on a comparison of the properties and sequences, the bacterial catalases had earlier been divided into three groups (Loewen, 1997). Group one contains the monofunctional catalases, subdivided into two subgroups on the basis of heme content and subunit size. The members of the first subgroup are often called typical monofunctional catalases and include eukaryotic catalases. These are homotetramers of 55-65 kD subunits with one protoheme IX (heme b) per subunit, although dimeric and hexameric structures have been observed, as have varied pH and thermal sensitivities. This subgroup was further subdivided in the phylogenetic analysis (Klotz *et al.* 1997) into Group I and III. The second subgroup contains the atypical monofunctional catalases, with larger subunit sizes (80-84 kD) and cis-hydroxy spirolactone heme (heme d) as the prosthetic group (Murshudov *et al.* 1996). These larger enzymes exhibit significantly enhanced stability and retain activity at 70°C, in 7M urea or 1% SDS, and over a broad pH range from 3.0 to 11.0. This became Group II in the phylogenetic analysis. The second major group of bacterial catalases contains the catalase-peroxidases, which are most commonly homotetramers of 80 kD subunits and contain heme b as a prosthetic group, and which exhibit a relatively sharp pH dependency. The third group of bacterial catalases includes the non-heme, manganese-containing catalases which have remained largely uninvestigated with only one sequence recently becoming available (Igarashi, 1996). Mn-catalases can be inhibited by chloride, nitrate, nitrite, azide, and other singly charged anions, except cyanide. Their subunit sizes are smaller than in heme-containing catalases and are stable up to 80°C (Khangulov *et al.*, 1990; Kono

and Fridovich, 1983; Allgood and Perry, 1986). Recently, the dinuclear manganese centers of catalases from *Thermus thermophilus* and *Lactobacillus plantarum* have been investigated (Ivancich, *et al.*, 1995; Meier *et al.*, 1996). Some spectroscopic studies have focused on the electronic structure of the active site and its relation to catalysis within the Mn-catalases.

The catalase reaction mechanism

The decomposition of hydrogen peroxide by catalase has been the object of study for over 150 years, and occurs by two separate and consecutive two-electron transfers as shown below (8)(9)(Chance, 1954; Fita and Rosemann, 1985, Ortiz de Montellano, 1992):



Fita and Rosemann have modeled a detailed mechanism for the formation and reduction of the methyl hydroperoxide catalase compound I. A suitably positioned distal histidine (His74 in BLC) and a second distal residue (arginine in peroxidases, asparagine in catalases (Asn147 in BLC)) are important for compound I formation and heterolytic peroxide cleavage. The initial step in the formation of compound I is the entrance of the peroxide molecule to the heme crevice on the heme's distal side. The peroxide is sterically constrained to move between the His-74 residue, which was biochemically confirmed to be critical in catalysis, and the Asn-147 residue, which is located in the active site close to the heme and His-74, before interacting with the heme iron. These residues are

believed to orient the substrate via hydrogen bonding as the catalase-peroxide complex is produced.

An electron “push-pull” mechanism is then applied (Dunford 1991), with the initial push being the flow of two electrons toward the ferric heme iron from the deprotonated oxygen atom of the peroxide that is coordinated to the heme. The proton is extracted by the imidazole nitrogen of the His-74. This push is initially generated by the ferric iron in association with the phenolate group of the proximal Tyr-357. The subsequent pull comes as the cleavage of the O-O bond takes place, being generated by the electrostatic interactions of one peroxide hydrogen with the His-74 imidazole and the second peroxide hydrogen with the Asn-147 amine group. The hydrogen extracted by the imidazole ring of the histidine is then attached to the oxygen as electrons flow away from the heme, forming a molecule of water, and an oxo-iron heme species ($\text{Fe}^{\text{V}}=\text{O}$) (compound I). The first step of this reaction (reaction 8) is extremely rapid with H_2O_2 as the substrate, having a specific velocity constant of approximately $1.0 \times 10^7 \text{M}^{-1}\text{s}^{-1}$ per hematin enzyme (Nicholls and Schonbaum, 1963). The mechanism of compound I formation is also generally applicable to peroxidases (Ortiz de Montellano, 1992).

The form of compound I can be either an oxyferryl iron at a formal oxidation level of IV in conjunction with a π -cation porphyrin radical as in plant peroxidases (Dunford, 1991) and eukaryotic catalases (Dolphin *et al.*, 1971), or a protein radical structure as in yeast cytochrome c peroxidase (CCP) (Ortiz de Montellano, 1992; Miller *et al.*, 1992) and some other hemoproteins, such as

metmyoglobin (Gibson et al., 1958; Catalano et al., 1989; Davies, 1991) and hemoglobin (Davies and Puppo, 1992). The π -cation radical structure of compound I has been confirmed with electron paramagnetic resonance (EPR) and colourimetric techniques, as well as analysis of synthetic heme systems (Dolphin *et al.* 1971). More sensitive studies employing resonance Raman spectroscopy have further confirmed it is the predominant configuration in BLC and horseradish peroxidase (HRP) (Chuang and Van Wart, 1992; Palanappian and Turner, 1990).

While the formation of compound I by the two electron oxidation process is a well characterized reaction, the reduction of catalase compound I is mechanistically less clear. The two electron reduction mechanism of catalase compound I proposed by Fita and Rosemann (1985), assumes the two electron donor reducing agent is a molecule of ethanol, rather than H_2O_2 . The model reaction proceeds with the sterically constrained ethanol being positioned via coordination of its C2 hydrogen to the oxyferryl heme oxygen and the His-74 and Asn-147 side chains. Extraction of the hydrogen from the C2 carbon by the oxo-iron oxygen weakens the oxo-iron bond, and increases the nucleophilic character of the His-74 imidazole nitrogen. The remainder of this process is still unclear. The catalytic reaction would likely be similar, with the obvious feature that the H_2O_2 is less sterically constrained which would allow a faster reaction rate and O_2 evolution. It is known that catalases prefer the two-electron reduction, instead of two one electron steps which has a much lower rate and forms compound II species in the process. The inactive peroxide compound II in which the iron

remains ferryl, but the porphyrin radical has been lost, may be formed through electron transfer from an endogenous donor on the apoprotein, or via addition of the appropriate one electron reductants to compound I.

Properties of HPII

Hydroperoxidase II (HPII) from *Escherichia coli*, is a Group II, or large subunit, catalase. Purification and physical characterization initially concluded that HPII was a hexamer of 84.2 kD subunits (Loewen and Switala 1986). The presence of heme d prosthetic groups was confirmed later (Chiu *et al.*, 1989). The subunit is encoded by the gene *katE*, which is located at 37.8 minutes on the *E. coli* chromosome (Loewen, 1984). The nucleotide sequence of the gene encodes a predicted protein of 753 amino acids with significant similarity to the typical shorter catalases from several plant, mammalian, and fungal sources (von Ossowski *et al.*, 1991). Like the typical catalases, HPII is active over a broad pH range (pH 4-11) with two optima at pH 6.8 and pH 10.5 (Meir and Yagil, 1985; Loewen and Switala, 1986). Unlike typical catalases, it exhibits enhanced stability at 70°C, in 7M urea or in 0.1% SDS (Meir and Yagil, 1985; Loewen and Switala, 1986). It remained for the resolution of the crystal structure to reveal that HPII actually exists as a homotetramer like typical catalases (Bravo *et al.*, 1995)

Regulation of HPII synthesis

During exponential growth, *E.coli* HPII is expressed at a low level in nutrient-rich medium, but is expressed at elevated levels in nutrient-poor medium. Expression reaches maximal levels eight- to ten- fold above base levels as cells enter stationary phase. This increase in HPII expression is coordinated with the expression of more than fifty other proteins as part of the *rpoS* regulon (Loewen and Triggs, 1984; Ossowski *et al.*, 1991; Loewen and Hengge-Aronis 1994). Only indirect evidence suggests the involvement of additional transcription factors (Mulvey *et al.*, 1990; Meir and Yagil 1990).

RpoS is an alternative σ transcription factor for RNA polymerase (Mulvey and Loewen, 1989), also referred to as KatF, σ^{38} and σ^S . In *E.coli*, σ^S controls the expression of a large number of genes involved in cellular stress responses including starvation, osmotic stress, acid shock, cold shock, heat shock and the transition to stationary phase (Loewen *et al.*, in press). Over 50 genes are under the control of σ^S , including *katE*. The synthesis of σ^S is controlled by mechanisms affecting transcription, translation, proteolysis and formation of the holoenzyme complex. Transcriptional control of *rpoS* involves ppGpp and polyphosphate as positive regulators (Gentry *et al.* 1993; Chesbro 1988; Lange *et al.* 1995; Shiba *et al.* 1997), and CRP-cAMP and *oxyS*-RNA as negative regulators (Lange and Hengge-Aronis 1991; 1994; McCann *et al.* 1993; Altuvia *et al.* 1997). Translational control of *rpoS*-mRNA involves a cascade of interacting factors including Hfq, H-NS, *dsrA*-RNA, LeuO and *oxyS*-RNA, all of which seem to modulate the stability of a region of secondary structure in the ribosome binding region of *rpoS* mRNA (Muffler *et al.*, 1997b; Barth *et al.*, 1995; Sledjeski

et al., 1996; Klauck *et al.* 1997; Zhang *et al.*, 1998). σ^S is sensitive to proteolysis by ClpPX in a reaction that is promoted by RssB and inhibited by the chaperone DnaK (Schweder *et al.*, 1996; Muffler *et al.*, 1997a; Muffler *et al.*, 1997c), and its activity is modulated by trehalose and glutamate (Kusano and Ishihama 1997).

Through these factors, environmental conditions change σ^S levels and activity. For example, carbon, phosphate or nitrogen starvation will result in the onset of the stationary phase of growth, causing changes of CRP-cAMP, ppGpp, trehalose, UDP-glucose and serine lactone levels, all of which may enhance σ^S expression (Gentry *et al.*, 1993; Lange and Hengge-Aronis 1994; Zgurskaya *et al.*, 1997). Acid shock of several organisms causes a RssB dependent induction of the synthesis of about 50 σ^S -dependent proteins (Bearson *et al.*, 1996; Gordon and Small 1993; Small *et al.*, 1994). Heat shock causes a DnaK-dependent induction of σ^S (Muffler *et al.*, 1997a). Finally, high osmolarity causes an increase in σ^S levels involving H-NS and RssB factors (Muffler *et al.*, 1996; Pratt and Silhavy 1996). This incomplete regulatory picture of σ^S indicates the complexity of the direct and indirect response of σ^S , and as a result, HPII, to environmental factors.

A single transcription start site was demonstrated at nucleotides -53/54 (relative to the translation start site) by primer extension analysis (Tanaka *et al.*, 1997). Immediately up-stream is a putative -10 sequence TATAGT which is similar to both the proposed σ^S promoter consensus sequence CTATACT and the housekeeping σ^D sequence, TATAAT (Hiratsu *et al.*, 1995, Espinosa-Urgel *et al.*, 1996). Espinosa-Urgel has proposed an element of curvature in the DNA

upstream of the promoter as an ancillary element that compensates for the absence of a -35 sequence in σ^S -dependent genes. Curvature may be a factor in *katE* gene transcription because a specific -35 sequence appears to not be necessary for expression of this gene.

Structure of typical catalase: BLC (bovine liver catalase)

To date, the three-dimensional structures of one eukaryotic, three bacterial and two fungal catalases have been solved. These are the bovine liver catalase (Murthy *et al.*, 1981), the *Proteus mirabilis* KatA (Gouet, 1993; Gouet *et al.*, 1995), the catalase of *Micrococcus luteus* (Yusifov *et al.*, 1989; Murshudov *et al.*, 1992), *E coli* HPII (Bravo *et al.*, 1995), *Penicillium vitale* catalase (Vainshtein *et al.*, 1986; Melik-Adamyanyan *et al.*, 1986; Murshudov *et al.*, 1996) and catalase A from *Saccharomyces cerevisiae* (Berthet, *et al.*, 1997). All of these were determined in large part by molecular replacement using BLC as a model, and have shown extensive structural similarity with the mammalian enzyme (Murthy *et al.*, 1981; Reid *et al.*, 1981; Melik-Adamyanyan *et al.*, 1986), the structure of which was first resolved at 2.5 Å resolution (Murthy *et al.*, 1981; Reid *et al.*, 1981) and later refined to 2.0 Å (Fita and Rossmann, 1985).

The subunit of BLC has 506 residues whose structure has been subdivided into four principal domains (Fita and Rossmann, 1985). These include an amino terminal extension "arm" (residues 1-70) containing two α -helices (α_1 and α_2), followed by a core domain (residues 76 - 320) forming an eight stranded β -barrel region consisting of two four-stranded anti-parallel β sheets (β_1 to β_4 and

β_5 to β_8) intercalated with α -helices (α_3 to α_7). The amino acids forming the active site (His74, Asn147, and Tyr357) are all located in this domain. A wrapping domain (residues 321-436) has little distinct secondary structure apart from an "essential" α helix (α_9), and the carboxy terminal domain (residues 437-506), contains four α helices (α_{10} to α_{13}) on the outer edge of the subunit molecule. Each catalase subunit in BLC can bind one molecule of NADPH (Kirkman and Gaetani, 1984) in the region near the "hinge" between two subunits. In addition there is a "knotting" of 25 residues of the amino terminus of one subunit through a loop in the wrapping domain of an adjacent subunit. Two knotted dimers form a roughly dumbbell shaped tetrahedral structure (Ruis, 1979; Fita and Rossman, 1985). The tightly bound NADPH has been detected in most typical catalases including those from human erythrocytes, bovine liver, dog (Kirkman and Gaetani, 1984), *Proteus mirabilis* (Jouve *et al.*, 1986 and 1989; Gouet *et al.*, 1995), *Micrococcus lysodeikticus* (Yusifov *et al.*, 1989) and *Saccharomyces cerevisiae* (Hillar *et al.*, 1994).

Structure of HP11

The crystal structure of catalase HP11 from *E.coli* was originally determined to 2.8 Å resolution (Bravo *et al.*, 1995) and more recently refined to 1.9 Å (Bravo, J. *et al.*, 1999). The HP11 subunit is 753 residues in length and contains a core of approximately 500 residues, with high structural similarity to the small subunit heme catalases, including BLC. To this core are added extensions of 75 to 80 amino acids and 180 amino acids at the N- and C- termini, respectively. Four domains have been identified within one subunit. Of these,

the N-terminal domain contains the first 79 residues in a largely disordered structure with two small α -helices involving residues 52-57 and 62-71. The interwoven structure described in BLC is enhanced in HP11 with 80 N-terminal residues inserted through a loop formed in the hinge region (Bravo *et al.*, 1997). This creates a very tightly associated structure that may in part explain the enhanced stability of the enzyme. The HP11 core domain (residues 80 to 433) has a highly conserved structure consisting of a β -barrel and α -helices. A wrapping domain is formed by residues 434-600 with a structure similar to that of BLC, although extended in length. This domain links to the C-terminal domain and loops over top of the N-terminus. The C-terminal end of HP11 (residues 600 to 753) contains four α -helices and eight β -strands and interacts almost exclusively with residues from the same subunit. This domain resembles the flavodoxin domain found in a number of nucleotide binding enzymes, but nucleotide binding has never been demonstrated in HP11. To date, the flavodoxin-like region in catalases has only been detected in HP11 and PVC, and is the major topological distinction between the large and small subunit enzymes.

The flavodoxin-like region is situated such that it blocks what would be the entrance to the substrate access channel in BLC. However, dimer formation results in a revised channel that is lengthened to 50 Å being located along the interface of the C-terminal domain and core region of associated subunits. The larger channel restricts access to the active site of substrates larger than H₂O₂. This may also prevent compound II formation and make NADPH binding redundant. The role of the extended sequences has been investigated through

the construction of truncated HP11 mutants (Sevinc *et al.*, 1998). Removal of the complete C-terminal domain and/or the N-terminal extension, prevents the accumulation of any enzyme probably through a disruption of the folding pathway. In fact the removal of more than nine C-terminal residues or eighteen N-terminal residues reduced the accumulation of active enzyme, emphasizing the importance of these regions in the folding pathway to create a protease resistant, stable structure.

One structural modification found in HP11 involves the blockage of the sulfhydryl group of cys438, one of the only two cysteines in HP11 (von Ossowski *et al.*, 1993). A hemithioacetal structure has been proposed for the blocking group, but further work is required to confirm the structure (Sevinc *et al.*, 1995). Several other intriguing peculiarities have been revealed within HP11 structure which will be introduced in the following sections.

Structural features of bovine liver catalase

Protoheme, the prosthetic component of BLC, interacts with the protein primarily with non-polar-side chains through van der Waals' forces. The propionate groups of heme are involved in a network of ionic interactions and hydrogen bonding. The heme pocket of BLC is very hydrophobic in character, with the distal side of the heme primarily defined by a surrounding β barrel domain "wall", which also interacts with the porphyrin pyrrole rings I, II, III. In BLC, the distal side of the heme with the essential His74 situated above the ring III also defines the catalytic site, into which the main heme channel opens. There

are several residues which are thought to have functional and /or structural importance including the distal side, His74, Ser113, Phe160, Phe152, Val173 and Asn147. On the proximal side of the heme, residues His217, Asp347, Arg353, Val145, Pro335 and Tyr357 have been ascribed important roles. The important proximal residues are all associated with the $\alpha 9$ helix which lies almost parallel to the heme plane, including Tyr357 which is the proximal ligand to the heme iron. A tyrosine phenolate group serving as the proximal ligand is unusual in hemoproteins other than catalase, with this position usually occupied by histidine (Dunford, 1991; Bosshard *et al.*, 1991).

Heme binding in HP11

Heme groups are deeply buried inside the HP11 tetramer in locations equivalent to those in BLC (Bravo *et al.*, 1995). The structure of the heme pocket, both on the distal and proximal sides, is well conserved. The essential residues in BLC (His74, Ser113, Asn147, Arg353 and Tyr357) can be superimposed on residues His128, Ser167, Asn201, Arg411 and Tyr415 in the structure of HP11. In addition, the solvent structure of BLC is well conserved in HP11. Despite this high level of heme pocket structural homology, there are significant differences in the heme groups. The HP11 heme is oxidized to a cis-hydroxyspirolactone on ring III (Murshudov *et al.*, 1996), and it is 'flipped' 180° around the axis defined by the α - γ meso carbon atoms with respect to that reported for BLC (Bravo, *et al.*, 1995). This results in the relative positions of rings I and IV interchanging with rings II and III, respectively, and in a change in the relative positions of the vinyl and methyl substituents on rings I and II. Based on the interaction with methyl

and vinyl groups in heme, the residues which govern heme orientation appear to be Ile274 and Pro356 (Bravo, *et al.*, 1995), and this has been partially confirmed by site-directed mutagenesis studies (Sevinc *et al.*, 1998). Other residues determining heme binding are the subject of a continuing investigation.

Due to the large degree of homology between the heme environments of BLC and HP11, the formation of compound I and its reduction to free enzyme by two-electron donors, such as H₂O₂, probably follows similar steps as described above and involves equivalent residues. Wild type HP11 catalase exhibited only 15% the activity of BLC per heme in one report (Obinger *et al.*, 1997) and 30% in a second (Bravo *et al.* 1998). The differences in activity may be correlated with differences in the peroxide entry channel, and recent results (Sevinc *et al.* 1999) have shown that enlarging a second channel in the Arg260Ala mutant enzyme increased activity of HP11.

The mechanism of catalysis involved in the heme modification in HP11 has been investigated, revealing that the *cis*-hydroxylation of protoheme is catalyzed by HP11 in a reaction that uses hydrogen peroxidase as a substrate and requires residues His128 and Asn201 (Loewen, *et al.*, 1993; Obinger *et al.*, 1997). A novel covalent bond between N_δ of His392 and C_β of Tyr415 was identified by electron density mapping of HP11 and confirmed by matrix-assisted laser desorption/ionization mass spectrometry analysis of tryptic digest mixtures (Bravo *et al.*, 1997a). The linkage was found only in HP11 subunits where the heme b to heme d conversion has also occurred, and a mechanistic relationship between the autocatalytic conversion of heme b to heme d and the formation of

the His392-Tyr415 bond was proposed (Bravo *et al.*, 1997a) (Fig 1.1). The mechanism involves the generation of compound I (containing an oxo-Fe^{IV} and a porphyrin π cation radical) and water in a first step that requires the active site residues His128 and Asn201 (Fig. 1.1A). A second H₂O₂ may then approach the essential Tyr415 through a cavity on the heme's proximal side, and may be oriented by hydrogen bonding with one or more of the adjacent residues Ser414, Thr418, or Gln419 (Fig. 1.1B). Gln419, located in the 9th helix of HP11, is involved in an important hydrogen bond matrix with heme d to stabilize it. (Murshudov *et al.*, 1996), and it is known that His395 forms hydrogen bonds with residues H392 and Asp197 (Bravo, J. *et al.*, 1999). H395 and D197 may be involved with extracting a proton from the N_ε of His392. This causes the N_δ of His392 to attack the C_β of Tyr415 which in turn attacks the H₂O₂ molecule to form water and hydroxide ion (Fig. 1.1C). The hydroxide ion reacts with the porphyrin π cation radical to produce a neutral radical. The subsequent transfer of one electron from the heme to the oxo-iron complex generates a cation which facilitates the cyclization of the propionate group into the spirolactone (Fig. 1.1D). The net effect of this reaction is that oxygen in the oxy-iron complex of compound I is converted to water, resulting in two H₂O₂ molecules being converted to three molecules of water, one hydroxyl group on the heme to form heme d and the His-Tyr bond.

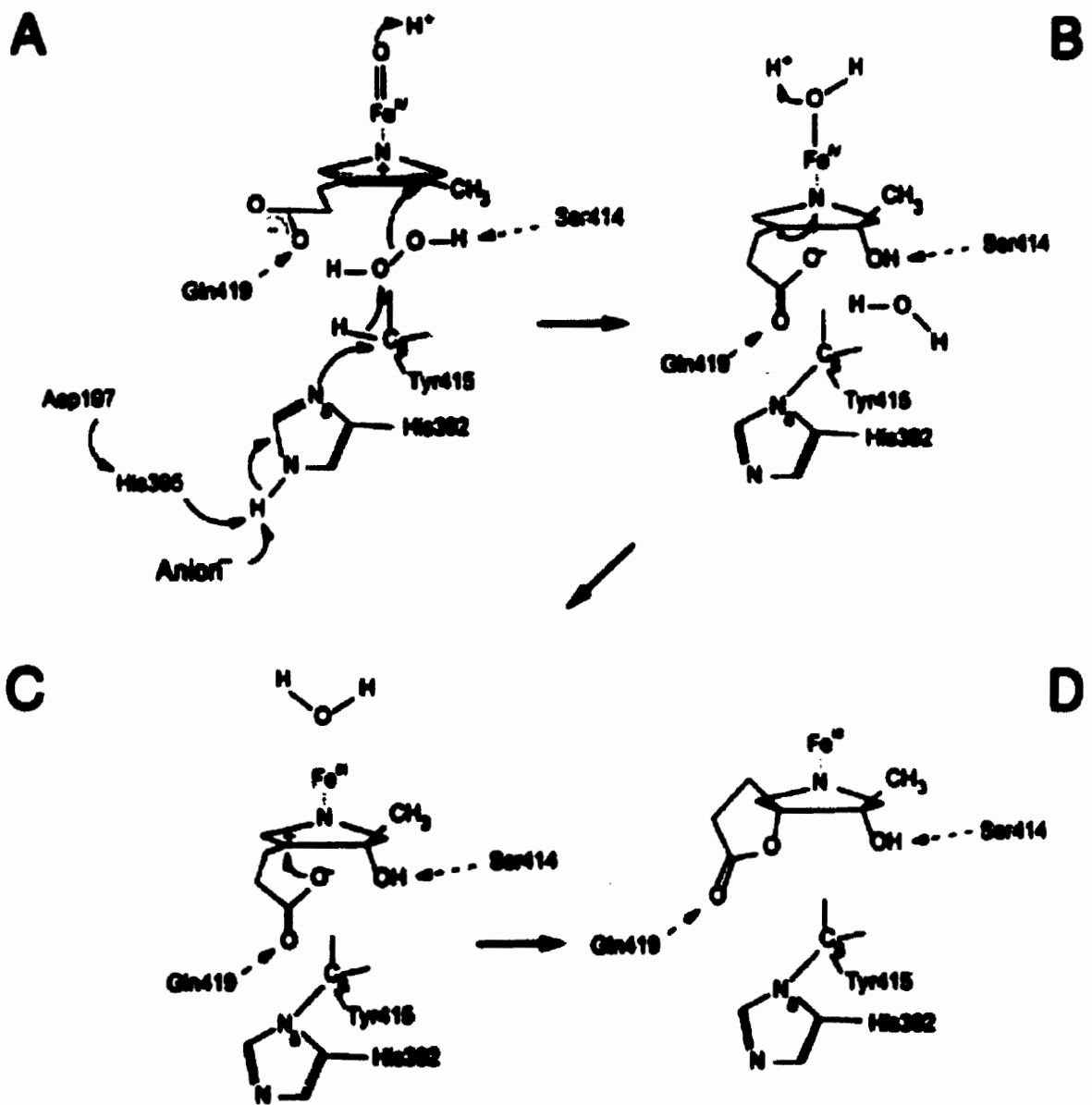


Figure 1.1. A proposed mechanism coupling the formation of the His-Tyr bond to the oxidation of ring III of the heme in HPII of *E. coli*. (Bravo, J. *et al.*, 1997)

Thesis objective

The goal of the research presented here was to determine whether and how the protein conformation of HPII in the vicinity of the heme prosthetic group dictates the conversion of heme from protoheme to heme d, and how these amino acid residues function. This was accomplished by individual amino acid modifications using site-directed mutagenesis and a characterization of the properties of these mutant enzymes. The amino acids targeted include His392, His395, Asp197 and Gln419, all proximal side residues. It was hoped that this project would broaden our understanding of the role of individual amino acids in the topography of proteins with respect to catalysis.

2. EXPERIMENTAL PROCEDURE

2.1. *Escherichia coli* STRAINS, PLASMIDS AND BACTERIOPHAGE

E. coli strain CJ236, NM533, UM255 and JM109 were used (Table 2.1). *E. coli* CJ236 served as the host for plasmid pKS⁻H-E, pKS⁺E-C and for the generation of uracil-containing single-stranded DNA for use in site directed *in vitro* mutagenesis. *E. coli* NM522 was used for most cloning and plasmid maintenance. *E. coli* JM109 was used for production of plasmid DNA for single stranded DNA sequencing. *E. coli* UM255 was used for the expression of catalase proteins.

Helper bacteriophage R408 was employed in the generation of single stranded DNA template for use *in vitro* mutagenesis.

The *katE* gene encoding HP11 catalase was originally cloned into pKS⁺ to generate the plasmid pAMkatE72 (von Ossowski *et al.*, 1991). Two subclones (pKS⁻H-E and pKS⁺E-C) and pAMkatE72 were used as source of partial or complete *katE* gene.

2.2. GROWTH MEDIA, CONDITIONS AND CULTURE STORAGE

LB (Luria-Bertani) Medium (Miller, 1972)

Per litre:	Bacto-tryptone	10 g
	Bacto-yeast extract	5 g
	NaCl	5 g
Solid media:	Bacto-agar	14 g

Table 2.1. Summary of *E. coli* strains, plasmids and bacteriophage used in project.

Name	Genotype	Source
<u>E.coli Strains</u>		
CJ236	<i>dut1 ung1 thi-1 relA1/pCJ105/• cam^rF'</i>	Kunkel <i>et al.</i> , 1987
NM522	<i>supE Δ(lac-proAB) hsd-5</i> [F' <i>proAB lac^q lacZΔ15</i>]	Mead <i>et al.</i> , 1985
UM255	<i>pro leu rpsL hsdM hsdR endI lacY katG2</i> <i>katE12::Tn10 recA</i>	Mulvey <i>et al.</i> , 1988
JM109	<i>recA1 supE44 endA1 hsdR17 gyrA96</i> <i>relA1 thiΔ (lac-proAB)</i>	Yanisch-Perron <i>et al.</i> , 1985
<u>Plasmids</u>		
pAMkatE72 (pKS ⁺ Pst I - Cla I, <i>katE</i> clone)	Amp ^r	von Ossowski <i>et al.</i> , 1991
pKS ⁺ EcoR I - Hind III (subclone II)	Amp ^r	von Ossowski <i>et al.</i> , 1991
pKS ⁺ EcoR I - Cla I (subclone III)	Amp ^r	von Ossowski <i>et al.</i> , 1991
<u>Bacteriophage</u>		
R408 (helper phage)		Stratagene

All *E. coli* strains used in this study were routinely grown in LB medium (both liquid and solid form). Ampicillin was added to a final concentration of 100µg/ml for liquid medium and solid medium when selecting for plasmid-containing cells. Chloramphenicol (40mg/ml) was also added to liquid medium in order to maintain the episome for the growth of strain CJ236.

R-top agar

Per liter:	Yeast extract	1 g
	Tryptone	10 g
	NaCl	8 g
	Agar	8 g

After autoclaving, 2 ml 1M CaCl₂, 3.36 ml 30% Glucose is added.

R-top agar was used to spread cells on selective LB medium plates after transformation with plasmid.

All *E. coli* strains, in liquid and on solid media, were grown at 37°C unless stated otherwise. Liquid cultures were grown with vigorous aeration on reciprocating or gyrotory shakers. Estimates of cell density were determined by converting the cell turbidity values determined spectrophotometrically at λ=600nm to Klett values ($A_{600} \times 168.6 - 34.7$) where Klett 100= 0.16 mg dry cell weight.

E. coli cultures were normally stored at -60°C in 8% (v/v) dimethyl sulfoxide (DMSO). Phage R408 was stored at 4°C in culture supernatant.

2.3. SITE-DIRECTED MUTAGENESIS STRATEGY

Site-directed point mutations on *katE* were generated according to the *in vitro* mutagenesis protocol described by Kunkel *et al.* (1987). Target bases of the

katE gene are labeled in Figure 2.1. The sequences of oligonucleotides used in mutagenesis construction are listed in Table 2.2. Uracil-containing single-stranded DNA obtained from the proper subclones of *katE* gene was extracted from *E.coli* CJ236 and annealed to phosphorylated oligonucleotides. The complementary strand containing the synthesized mutations was generated *in vitro* and then transformed into *E.coli* NM522 wherein the uracil-containing strand was degraded. Plasmid was then recovered from *E.coli* NM522 and transformed into *E.coli* JM109 for sequencing. Once the target mutant was identified, the complete sequence of the subclone was determined to ensure that no other base changes had occurred. The appropriate fragment of mutant subclone was inserted into pAMkatE72 to reconstruct the complete mutant *katE*, and transformed into *E.coli* NM522, then *E.coli* UM255, and lastly *E.coli* JM109. The insert was sequenced again to verify the nature of the mutant sequence. Crude protein extracts from confirmed clones were recovered from *E.coli* UM255 and examined by SDS-PAGE. Clones expressing HP11-like protein were then grown in large scale for enzyme purification and characterization.

2.3.A. Preparation and isolation of oligonucleotides

Oligonucleotides required for *in vitro* mutagenesis and DNA sequencing were synthesized by Mr. J. Switala on a PCR-Mate Synthesizer (Applied Biosystems, Inc.) according to the method suggested by the manufacturer.

Figure 2.1. The DNA sequence of the insert of *katE* gene within pAMkatE72. The sequences of the mutagenic primers, sequencing primers and the restriction enzymes used in cloning are also shown (modified from von Ossowski *et al.*, 1991).

Pst I

1 CTGCAGCCTT TCTTTAAAAG AGTCGAAAGC CAGGCTTTTA ATATTTAAAT CACCATAATT
61 ACTCTGTATT AAGTTTGTAG AAAACATCTC CCGCCTCATA TTGTTAACAA AATTATTATC
121 TCATTTAAAT CTAAGTCATT TACAATATAA GTTTAAGAGC GACGCCACAG GATGAACAT
181 CAAAAATAGC TCATCATGAT TAGCAAAACT TAACCATTTT AAAATAAATA AACAAATAAA
241 GAAAAAGAT CACTTATTTA TAGCAATAGA TCGTCAAAGG CAGCTTTTTG TTACAGGTGG
301 TTTGAATGAA TGTAGCAACG AAATACAGAA TTTTCAGTCA TGTAACCCC GGCAAACCGG
361 GAGGTATGTA ATCCTTACTC AGTCACTTCC CCTTCCTGGC GGATCTGATT TGCCCAACGT
421 TGGGCAGATT CAGGCACAGT AAACGCCGGT GAGCGCAGAA ATGACTCTCC CATCAGTACA
481 AACGCAACAT ATTTGCCACG CAGCATCCAG ACATCAGAA ACGAATCCAT CTTTATCGCA
541 TGTTCTGGCG GCGCGGGTTC CGTGCGTGGG ACATAGCTAA TAATCTGGCG GTTTTGCTGG
601 CGGAGCGGTT TCTTCATTAC TGGCTTCACT AAACGCATAT TAAAAATCAG AAAAACTGTA
661 GTTTAGCCGA TTTAGCCCCT GTACGTCCC G TTTGCGTGT ATTTCATAAC ACCGTTTCCA
721 GAATAGTCTC CGAAGCGGGA TCTGGCTGGT GGTCTATAGT TAGAGAGTTT TTTGACCAA
781 ACAGCGGCC TTTTCAGTAAT AAATTAAGGA GACGAGTTCA ATGTCGCAA CATAACGAAAAG

1 M S Q H N E K 7

842 AACCCACAT CAGCACCAG TCACCACTA CACGATTCC AGCGAAGCG AAACCGGGG ATGGAC
N P H Q H Q S P L H D S S E A K P G M D 27
902 TCACTGGCA CCTGAGGAC GGCTCTCAT CGTCCAGCG GCTGAACCA ACACCGCCA GGTGCA
S L A P E D G S H R P A A E P T P P G A 47
962 CAACCTACC GCCCCAGGG AGCCTGAAA GCCCTGAT ACGCGTAA CAAAACTT AATTCT
Q P A P G S L K A P D T R N E K L N S 67
1022 CTGPAAGAC GTACGAAA GGCAGTGAA AATTATGCG CTGACCACT AATCAGGGC GTGCGC
L E D V R K G S E N Y A L T T N Q G V R 87
1082 ATCGCCGAC GATCAAAAC TCACTGCGT GCCGGTAGC CGTGGTCCA ACGCTGCTG GAAGAT
I A D D Q N S L R A G S R G P T L L E D 107
1142 TTTATTCTG CGCGAGAAA ATCACCCAC TTTGACCAT GAGCGCAT CCGGAACGT ATTGTT
F I L R E K I T H F D H E R I P E R I V 127

Hind III

1202 CATGCACGC GGATCAGCC GCTCACGGT TATTTCCAG CCATATAAA AGCTTAAGC GATATT
H A R G S A A H G Y F Q P Y K S L S D I 147
1262 ACCAAAGCG GATTTCCCTC TCAGATCCG AACAAAATC ACCCCAGTA TTTGTACGT TTCTCT
T K A D F L S D P N K I T P V F V R F S 167
1322 ACCGTTACG GGTGGTGCT GGCTCTGCT GATACCGTG CGTGATATC CGTGGCTTT GCCACC
T V Q G G A G S A D T V R D I R G F A T 187

D197A: -----GCC----->

D197S: -----AGC----->

1382 AAGTTCTAT ACCGAAGAG GGTATTTTT GACCTCGTT GGCAATAAC ACGCCAATC TTCTTT
K F Y T E E G I F D F V G N N T P I F F 207
1442 ATCCAGGAT GCGCATAAA TTCCCCGAT TTTGTTTAT GCGGTAAAA CCAGAACCG CACTGG
I Q D A H K F P D F V H A V K P E P H W 227
1502 GCAATTCCA CAAGGGCAA AGTGCCCCAC GATACTTTC TGGGATTAT GTTTCTCTG CAACCT
A I P Q G Q S A H D T F W D Y V S L Q P 247
1562 GAAACTCTG CACAACGTG ATGTGGGCG ATGTCCGAT CGCGGCATC CCCCAGT TACCGC
E T L H N V M W A M S D R G I P R S Y R 267
1622 ACCATGGAA GGCTTCGGT ATTCACACC TTCCGCTG ATTAATGCC GAAGGAAG GCAACG
T M E G F G I H T F R L I N A E G K A T 287
1682 TTTGTACGT TTCCACTGG AAACCACG GCAGGAAA GCCTCACTC GTTTGGGAT GAAGCA
F V R F H W K P L A G K A S L V W D E A 307
1742 CAAAACTC ACCGGACGT GACCCGGAC TTCCACCGC CGCGAGTTG TGGGAAGCC ATTGAA
Q K L T G R D P D F H R R E L W E A I E 327

EcoR I

1802 GCAGGCGAT TTTCCGGAA TACGAACTG GGCTTCCAG TTGATTCCT GAAGAAGAT GAATTC
A G D F P E Y E L G F Q L I P E E D E F 347

-----> F

1862 AAGTTCGAC TTCGATCTT CTCGATCCA ACCAACTT ATCCCGGAA GAAGTGGTG CCGGTT
K F D F D L L D P T K L I P E E L V P V 367

1922 CAGCGTGC GGCAAAATG GTGCTCAAT CGCAACCCG GATAACTTC TTTGCTGAA AACGAA
Q R V G K M V L N R N P D N F F A E N E 387

H392A: -----GCT----->

H392Q: -----CAG----->
H395A: -----GCT----->
H395Q: -----CAG----->

1982 CAGGCGGCT TTCCATCCT GGGCATATC GTGCCGGGA CTGGACTTC ACCAACGAT CCGCTG
Q A A F H P G H I V P G L D F T N D P L 407

Q419A: -----GCA----->
Q419H: -----CAT----->

2042 TTGCAGGGA CGTTTGTTC TCCTATACC GATACACAA ATCAGTCGT CTTGGTGGG CCGAAT
L Q G R L F S Y T D T Q I S R L G G P N 427

2102 TTCCATGAG ATTCGGATT AACCGTCCG ACCTGCCCT TACCATAAT TTCCAGCGT GACGGC
F H E I P I N R P T C P Y H N F Q R D G 447

Sph I

2162 ATGCATCGC ATGGGGATC GACACTAAC CCGGCGAAT TACGAACCG AACTCGATT AACGAT
M H R M G I D T N P A N Y E P N S I N D 467

2222 AACTGGCCG CGCGAAACA CCGCCGGGG CCGAAACGC GGCGGTTTT GAATCATAC CAGGAG
N W P R E T P P G P K R G G F E S Y Q E 487

2282 CCGGTGGAA GGCAATAAA GTTCGCGAG CGCAGCCCA TCGTTTGGC GAATATTAT TCCCAT
R V E G N K V R E R S P S F G E Y Y S H 507

2342 CCGCTCTG TTCTGGCTA AGTCAGACG CCATTTGAG CAGCGCCAT ATTGTCGAT GGTTC
P R L F W L S Q T P F E Q R H I V D G F 527

2402 AGTTTTGAG TTAAGCAAA GTCGTTCTG CCGTATATT CGTGAGCGC GTTGTGAC CAGCTG
S F E L S K V V R P Y I R E R V V D Q L 547

2462 GCGCATATT GATCTCACT CTGGCCCAG GCGGTGGCG AAAAAATCTC GGTATCGAA CTGACT
A H I D L T L A Q A V A K N L G I E L T 567

2522 GACGACCAG CTGAATATC ACCCCACCT CCGGACGTC AACGGTCTG AAAAAAGGAT CCATCC
D D Q L N I T P P P D V N G L K K D P S 587

2582 TTAAGTTTG TACGCCATT CCTGACGGT GATGTGAAA GGTCGCGTG GTAGCGATT TTA
L S L Y A I P D G D V K G R V V A I L L 607

2642 AATGATGAA GTGAGATCG GCAGACCTT CTGGCCATT CTCAAGCGC CTGAAGGCC AAAGGC
N D E V R S A D L L A I L K A L K A K G 627

2702 GTTCATGCC AA
ACTGCTC TACTCCCGA ATGGGTGAA GTGACTGCG GATGACGGA ACGGTG
V H A K L L Y S R M G E V T A D D G T V 647

2762 TTGCCATA GCCGCTACC TTTGCCGGT GCACCTTCG CTGACGGTC GATGCGGTC ATTGTC
L P I A A T F A G A P S L T V D A V I V 667

2822 CCTTGCGGC AATATCGCG GATATCGCT GACAACGGC GATGCCAAC TACTACCTG ATGGAA
P C G N I A D I A D N G D A N Y Y L M E 687

2882 GCCTACAAA CACCTTAAA CCGATTGCG CTGGCGGGT GACGCGCGC AAGTTTAAA GCAACA
A Y K H L K P I A L A G D A R K F K A T 707

2942 ATCAAGATC GCTGACCAG GGTGAAGAA GGGATTGTG GAAGCTGAC AGCGCTGAC GGTAGT
I K I A D Q G E E G I V E A D S A D G S 727

3002 TTTATGGAT GAACTGCTA ACGCTGATG GCAGCACAC CGCGTGTGG TCACGCATT CCTAAG
F M D E L L T L M A A H R V W S R I P K 747

3062 ATTGACAAA ATTCCTGCC TGATGGGAG CGCGCAATTGCG CCGCCTCAATG ATTTACATAG
I D K I P A 783

3122 TGCGCTTTG TTTATGCCG GATGCGCGT GAACGCCTTATC CGGCCTACAAA ACTGTGCAAA
3182 TTCAATATA TTGCAGGAA ACACGTAGG CCTGATAAGCGA AGCCATCAGGC AGTTTTGCGT
3242 TTGTCAGCA GTCTCAAGC GGCGGCAGT TACGCCGCCTTT GTAGGAATTAA TCGCCGGATG
3302 CAAGTTCA CGCCGATCT GGCAAACAT CCTCACTTACAC ATCCCGATAAC TCCCAACCG
3362 ATAACCACG CTGAGCGAT AGCACCTTT CAACGACGCTGA TGTCAACACAT CCAGCTCCGT
Cla I

3422 TAAGCGTGG GAAACAGTA AGCACTCTG ACGGATAGTATT ATCGAT

Table 2.2. Sequences of the oligonucleotides used for site-directed mutagenesis

mutagenesis of <i>katE</i> Name of Primer	Position within <i>katE</i>	Oligonucleotide sequence	Subclone used *
D197A (GAC → GCC)	1397-1420	5'- GAGGGTATTTTT <u>GCC</u> CTCGTTGGC	II
D197S (GAC → AGC)	1397-1420	5'- GAGGGTATTTTT <u>AGC</u> CTCGTTGGC	II
H 392A (CAT → GCT)	1985-2005	5'-GCGGCTTT <u>CGC</u> TCCTGGGCAT	III
H 392Q (CAT → CAG)	1985-2005	5'-GCGGCTTT <u>CAG</u> CCTGGGCAT	III
H 395A (CAT → GCT)	1996-2013	5'- TCCTGGGG <u>CTA</u> TCGTGCCG	III
H 395Q (CAT → CAG)	1996-2013	5'- TCCTGGGG <u>CAG</u> ATCGTGCCG	III
Q419A (CAA → GCA)	2066-2085	5'-ACCGATACAG <u>CA</u> ATCAGTCGT	III
Q419H (CAA → CAT)	2066-2085	5'-ACCGATAC <u>CA</u> TATCAGTCGT	III

* subclone II: pKS⁺EcoR I - Hind III of *katE* gene
subclone III: pKS⁺EcoR I - Cla I of *katE* gene (Table 2.1.)

Oligonucleotides were cleaved from the cartridge using 0.8 ml concentrated ammonium hydroxide and incubated at 55°C overnight. The sample was then lyophilized and resuspended in high pressure liquid chromatography (HPLC) grade distilled water and stored at -20°C. Oligonucleotide concentration was determined spectrophotometrically at $\lambda=260$ nm (1 OD unit equal to 40 $\mu\text{g/ml}$ single-stranded DNA) (Sambrook *et al.* 1989).

2.3.B. Uracil-containing single stranded DNA isolation

Single stranded DNA for site-directed mutagenesis was isolated and purified according to the method of Vieira and Messing (1987). 20 μl helper phage (10^{11} to $10^{12}/\text{ml}$) was added to plasmid containing cells in mid-log growth and grown 6-8 hours. After centrifuging the lysate twice for 2 minutes at 13,000rpm, 300 μl of 1.5 M NaCl and 20% Polyethylene glycol, 6000 (PEG) was added to 1.2 ml supernatant and mixed by inversion. The mixture was incubated 15 minutes at room temperature and centrifuged to pellet the phage particles. The pellet was resuspended in 200 μl of TE buffer. The mixture was extracted with 150 μl of phenol first, then 150 μl water saturated chloroform. The single stranded DNA was pelleted by centrifuging for 15 min after adding 150 μl , 7.5 M ammonium acetate (pH 7.5), 600 μl , cold 95% ethanol, and kept at -20°C for 20 min. The pellet was washed three times with 70% ethanol, dried in a vacuum line and kept at -20°C. Prior to use, the DNA was dissolved in distilled water.

2.3.C. Site-directed mutagenesis

Mutagenic primers were first phosphorylated by mixing 2 μl of ATP (100 mM), 18 μl dH₂O, 2 μl primer ($\text{OD}_{260} = 3.0-4.0 = 200-300$ pmol), 2.5 μl 10xT4

kinase buffer and 1 μ l T4 kinase. The mixture was incubated at 37°C for 30 to 45 minutes, and then for 5 minutes at 65°C. Based on established mutagenesis protocols (Kunkel *et al.* 1987; von Ossowski *et al.*, 1991), 2 μ l phosphorylated primer was annealed to 7 μ l ssDNA template in the presence of 1.5 μ l 20x SSC (3M NaCl, 300 mM NaCitrate) and 20.5 μ l dH₂O. This was incubated first at 73°C for 3 minutes and then at room temperature for 20 minutes. One μ l T7 DNA polymerase (~ 10,000U/ml), 2.5 μ l T4 DNA ligase, and 77 μ l synthesis mix (47 μ l dH₂O, 10 μ l 200mM HEPES (pH 7.8), 2 μ l 100mM DTT, 4 μ l 200mM MgCl₂, 10 μ l 10mM ATP and 4 μ l 50mM dNTPs (each 1:1:1:1)) were added to the annealing mixture and incubated on ice for 5 minutes, followed by incubation at room temperature for 5 minutes and then at 37°C for 3 hours. The reaction was stopped by the addition of 3 μ l TE buffer. Forty μ l of this mixture was used to transform competent *E.coli* NM522 cells .

2.3.D. Transformation

Transformation of *E. coli* was carried out as described by Chung *et al.* (1989) with modifications. Cells in early mid-log phase of growth (2-3 hours at 37°C) were harvested by centrifugation at 7,000g for 5 minutes (5 ml/tube) and made competent by resuspending in 0.1 M calcium chloride (0.5 ml/tube) for 30 minutes on ice. Plasmid DNA (1 μ l/tube) was added and incubated on ice for a further 30 minutes before heat shock at 42°C for 90 seconds. After allowing the cells to recover at 37°C in LB medium (1 ml/tube) for 1 hour without aeration, the mixture was added to 2.5 ml premelted R-top agar and instantly plated on Ampicillin-containing LB plates to grow overnight at 37°C.

2.3.E. Plasmid isolation and purification

Plasmid DNA isolation was conducted according to Sambrook *et al.* (1989) with modifications as described by Sevinc (1997).

2.3.F. Restriction endonuclease digestion of DNA

Plasmid DNAs were digested with restriction endonucleases (Life Technologies) at 37°C for 2.5-3 hours by mixing 1-10 µl DNA, 1 µl RNase (1 mg/ml), 1-2 µl optimal 10 x buffer, 0.5 µl restriction endonuclease and distilled water in a 10-20 µl final volume. After incubation, 3 µl stop buffer (40% (v/v) glycerol, 10 mM EDTA pH 8.0, 0.25% (w/v) bromphenol blue) was used to stop the reaction.

2.3.G. Agarose gel electrophoresis

Agarose gel electrophoresis of restriction endonuclease digested DNA was conducted as described by Sambrook *et al.* (1989). Agarose gels were prepared in 40 ml TAE buffer (40 mM Tris-acetate and 1 mM EDTA, pH 8.0, normally stored as 5x solution at room temperature) containing 1% (w/v) agarose using Bio-Rad Mini Sub DNA Cell horizontal electrophoresis trays (6.5 cm x 10 cm). The gel mixture was supplemented with 1 µl 4 mg/ml ethidium bromide immediately prior to gel casting. The gel was run at 40 mA constant current for 1 hour while submerged in TAE buffer. The molecular weight size marker used was the 1 Kb plus DNA ladder (GIBCO-BRL) and was prepared by adding 1 µl stock ladder to 3 µl stop buffer. DNA bands were visualized with ultraviolet light and photographed using a red filter and Polaroid Type 667 black and white film, or with the Bio-Rad Gel Doc 1000 system.

2.3.H. Single Stranded DNA sequencing

Single stranded DNA sequencing was conducted according to the method of Sanger *et al.* (1977) using the T7 sequencing kit (Pharmacia) according to the manufacturer's instructions, with electrophoresis conducted on 8% (w/v) polyacrylamide gels supplemented with 7M urea. Gels were dried and exposed to Kodak X-OMAT AR film overnight at room temperature to visualize DNA bands. Radioisotope used was [$\alpha^{32}\text{P}$] dATP (DuPont) (5-15 μCi).

2.3.J. DNA bands recovery

DNA bands excised from agarose gels were recovered and purified using the GENECLEAN DNA extraction kit (Bio/Can Scientific Inc.). For small DNA bands (< 1000 bp) a modification of the freeze-squeeze method was used. In this method, the frozen gel piece containing the desired DNA band was squeezed firmly, then incubated at 55°C for at least 10 minutes with an equal volume of 2% CTAB and 2M NaCl solution. The solution was extracted with an equal volume of chloroform and then combined with 2 volumes of 100% ethanol. After incubation at -60°C for one hour, the DNA was pelleted by centrifugation in a table top microcentrifuge at 4°C for 15 minutes and resuspended in TE buffer.

2.4. PROTEIN PURIFICATION

For large scale preparations, 10 μl frozen *E. coli* UM255 harbouring the desired pMZ plasmid was used to inoculate 50 ml LB broth supplemented with Amp and incubated at 28°C with shaking for 20-22 hours. The culture was transferred to 8-16 2 liter flasks (500 ml LB + Amp per flask) with final bacterial

inoculum concentration of $A_{600} = 0.01$. These cultures were incubated at 28°C with shaking for 22-24 hours. Cells were recovered by centrifugation at 8000 rpm for 15 minutes and resuspended in buffer KP (50 mM potassium phosphate buffer, pH7.0, 5 mM EDTA) using a ratio of 75 g cells per 400 ml buffer. Cells were disrupted using a French press at 20,000 psi and the debris removed by centrifugation at 12,000 rpm for 10 minutes. Proteins in the supernatant were precipitated by centrifugation at 12,000 rpm in a stepwise manner using 2.5% streptomycin sulfate and increasing (35%, 50%, and 60%) ammonium sulfate concentrations. Protein pellets from the 50% and 60% ammonium sulfate precipitates were combined and dissolved in 50-80 ml buffer KP. Ammonium sulfate precipitations at 30%, 40% and 50% were carried out and the precipitate with the highest specific activity was saved for further purification by anion exchange chromatography using DEAE Sephadex A-50 resin pre-equilibrated with buffer KP. HP11 was eluted with a NaCl gradient of 0.25 to 0.4M. Fractions recovered were assayed for catalase activity and absorbance at A_{280} , with fractions sharing peaks for both characteristics being pooled. These HP11 enriched fractions were concentrated under $\text{N}_{2(g)}$ with a protein concentrator (Amicon) to a final volume of 1-3 mL, and then dialyzed against buffer KP overnight prior to protein analysis. Small aliquots of the enzymes were stored at -70°C .

2.5. PROTEIN CHARACTERIZATION

2.5.A. Sodium dodecyl sulfate-polyacrylamide gel electrophoresis (SDS-PAGE)

SDS-PAGE was carried out according to Weber *et al.* (1972). Twenty to forty μg of each crude protein extract sample or 5-10 μg purified protein were mixed with equal volumes of sample buffer (per 10 ml: NaH_2PO_4 34 mg, Na_2HPO_4 102 mg, SDS 100 mg, 2-mercaptoethanol 100 μl , Urea 3.6 g) and 3 μl 1% bromophenol blue. Samples were run on an 8% polyacrylamide gel with 30-50 mA constant current in a vertical BIO-RAD Protean II electrophoresis system or 25 mA in a BIO-RAD Mini-Protean II cell. Samples were stained in staining solution (0.5 g/l Coomassie Brilliant Blue R-250 (Sigma), 30% ethanol and 10% acetic acid in water) and destained with repeated changes of the destaining solution (15% methanol, 7% acetic acid in water). The gel was dried on 3mm Whatman paper at 60°C in a slab gel dryer (Savant).

2.5.B. Catalase activity assay and Protein quantification

Catalase activity was determined by the method of Rorth and Jensen (1967) in a Gilson oxygraph equipped with a Clark electrode. One unit of catalase is defined as the amount of enzyme required to decompose 1 μmol H_2O_2 in 1 minute in a 60 mM H_2O_2 solution at 37°C, pH 7.0. Catalase activity (units/ml) was determined by adding 20-50 μl of appropriately diluted HPII protein to 1.8 ml 50 mM potassium phosphate buffer, pH 7.0 and 50 μl H_2O_2 (60 mM final concentration). Catalase activity was determined in whole cells using SM buffer (100 mM NaCl, 1 mM MgSO_4 , 20 mM Tris HCl, pH 7.6 and 100 mg/L gelatin).

Protein concentration (mg/ml) was estimated spectrophotometrically based on A_{280}/A_{260} ratios (Layne, 1957), and total cell dry weight estimated as described above (2.2. growth media, condition and culture storage). Specific activity (units/mg purified protein or units/mg whole cell weight) was calculated by dividing the activity/ml by protein concentration.

2.5.C. Inhibition studies

The effect of several inhibitors on HPII were studied, including CH_3ONH_2 , $\text{C}_2\text{H}_5\text{ONH}_2$, NH_2OH , NaCN and NaN_3 . Various concentrations of these inhibitors were incubated with HPII at 37°C for 1 min in KP buffer prior to the addition of H_2O_2 in the reaction cell to test enzyme activity. For spectral analysis, HPII was incubated with the various inhibitors for 3 hours at 37°C , and the absorption spectra determined from 350 to 750 nm.

2.5.D High Performance Liquid Chromatography

The detection of prosthetic groups in mutant HPII proteins was carried out according to the procedures of Loewen *et al.* (1993), the details of which have been described (Sevinc, 1997). The LKB HPLC system was used to detect the heme group at 370 nm extracted from HPII protein. Data were transferred to Lotus 123 and Freelance (Lotus) for preparation of elution profiles.

3. RESULTS and DISCUSSION

Section I: Construction of mutant catalase HPiIs

Catalase HPiI has previously been studied for the autocatalytic conversion of heme b to heme d in its prosthetic group (Loewen, *et al*, 1993). The discovery of a novel covalent bond between N_ε of His392 and C_β of Tyr415 in HPiI subunits led to the proposal of a mechanistic relationship between the conversion of heme b to heme d and the formation of the His392-Tyr415 bond (Bravo *et al.*, 1997a). In this study, the predicted roles of four proximal-side, heme-conversion related residues (Gln419, His392, His395, Asp197) in HPiI catalase were tested by mutation to either alanine or an oppositely charged amino acid. The organization of these four presumptive heme-conversion related residues in HPiI is shown in Figure 3.1.1.

The amino acid alterations in catalase HPiI were D197A, D197S, H392A, H392Q, H395A, H395Q, Q419A, Q419H and D197S/H395Q. Autoradiograms confirming the actual base changes in the DNA sequence for each amino acid substitution are presented in Figure 3.1.2. DNA fragments identified as having the proper base changes were recovered and inserted into pAMkatE72 to generate the mutant *katE* gene, which was then transformed into UM255 cells.

Section II: Purification of mutant catalase HPiIs

The mutant HPiI protein was purified as described in Experimental procedures. Purified preparations of the wild type and mutant HPiI catalases

Figure 3.1.1. Amino acids in the vicinity of heme d.

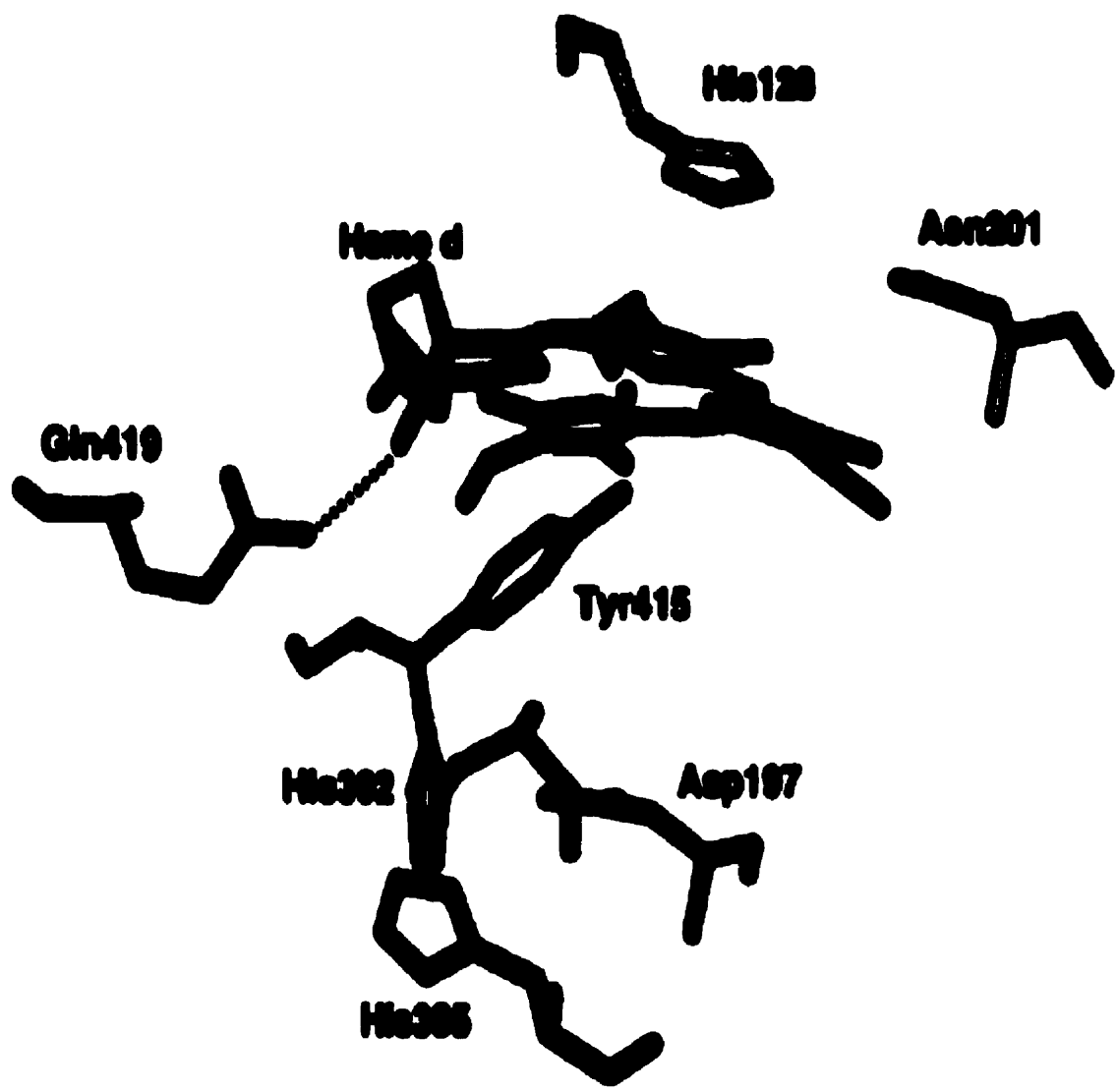


Figure 3.1.2. Autoradiograms of sequencing gels revealing base changes in the codon sites for Asp197, His392, His395, Gln419 in HPII catalase.

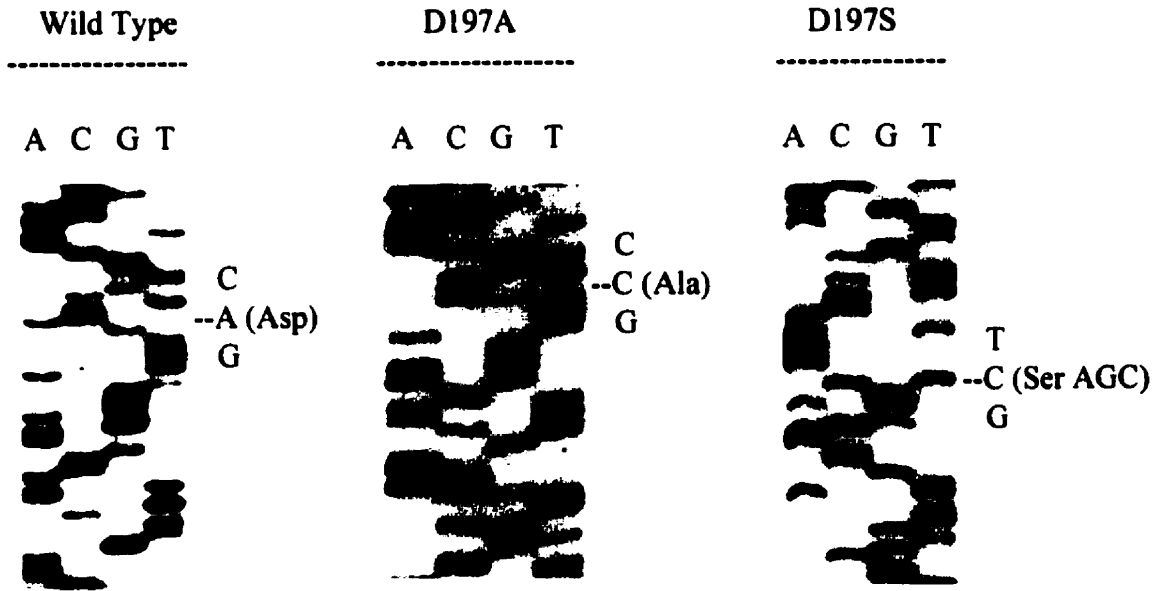
(1) The sequence of wild-type *katE* is shown on the left with sequences of the same region for the mutants D197A and D197S shown on the right. Base changes required for the replacement of Asp197 (GAC) in the wild type enzyme with the amino acids Ala (GCC), and Ser (AGC) are indicated.

(2) The sequence of wild-type *katE* is shown on the left with sequences of the same region for the mutants H392A and H392Q shown on the right. Base changes required for the replacement of His392 (CAT) in the wild type enzyme with the amino acids Ala (GCT), and Gln (CAA) are indicated.

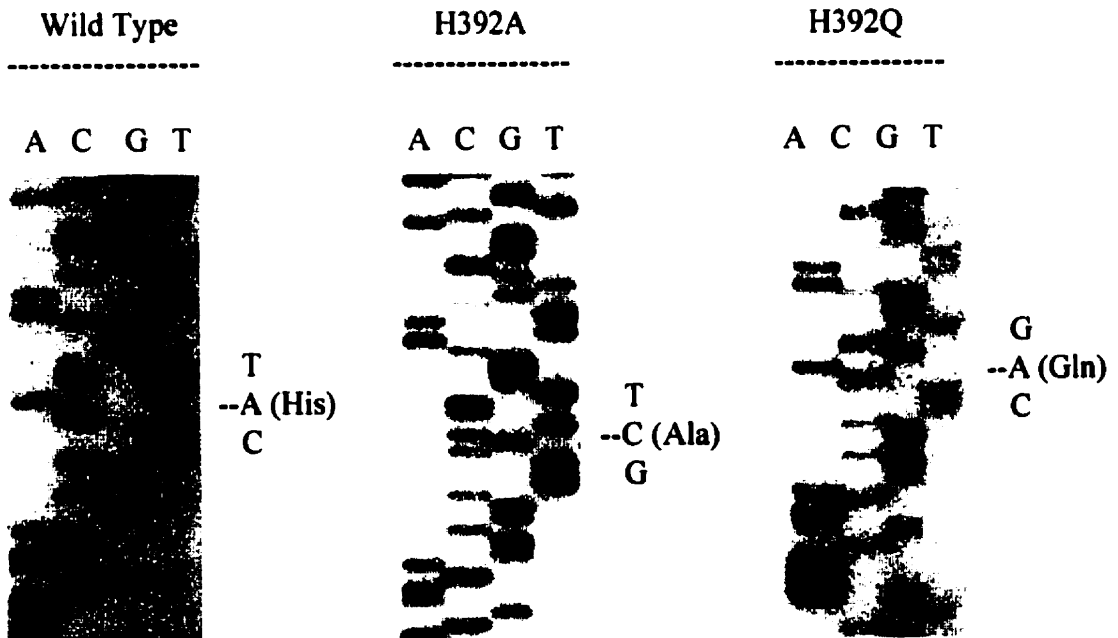
(3) The sequence of wild-type *katE* is shown on the left with sequences of the same region for the mutants H395A and H395Q shown on the right. Base changes required for the replacement of His395 (CAT) in the wild type enzyme with the amino acids Ala (GCT), and Gln (CAA) are indicated.

(4) The sequence of wild-type *katE* is shown on the left with sequences of the same region for the mutants Q419A and Q419H shown on the right. Base changes required for the replacement of Gln419 (CAA) in the wild type enzyme with the amino acids Ala (GCA), and His (CAT) are indicated.

(A) Asp197



(B) H392



(C) His395

Wild Type

A C G T



T
--A (His)
C

H395A

A C G T



T
--C (Ala)
G

H395Q

A C G T

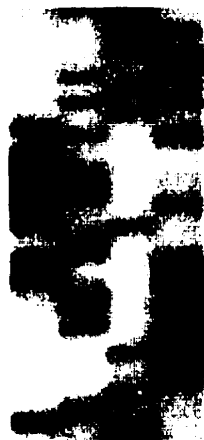


G
--A (Gln)
C

(D) Gln419

Wild Type

A C G T



A
--A (Gln)
C

Q419A

A C G T



A
--C (Ala)
G

Q419H

A C G T



T
--A (His)
C

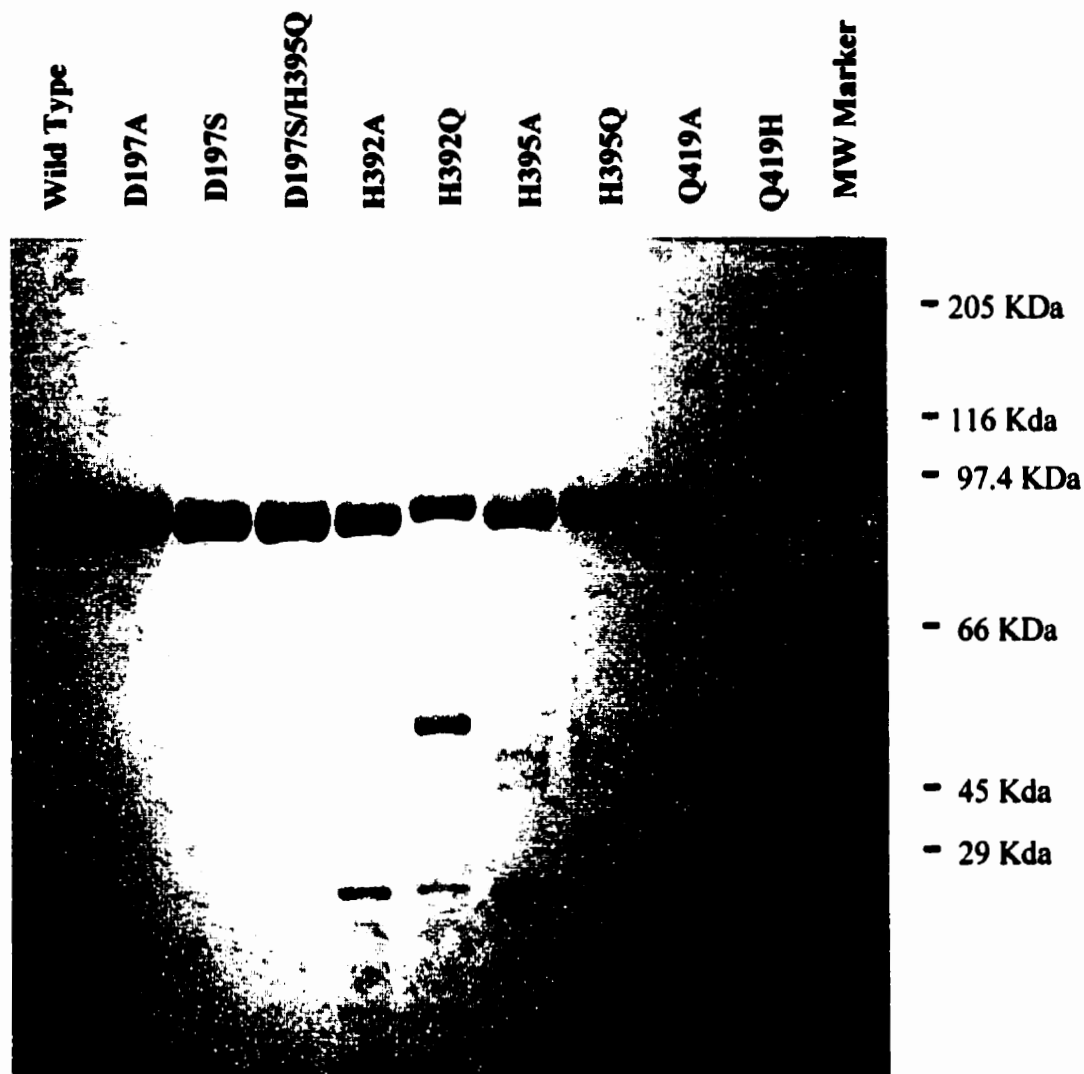


Figure 3.2.1. SDS-polyacrylamide gel electrophoresis analysis of various mutants of HP11 following purification. Samples of approximately 10 μ g were electrophoresed on an 8% gel and stained with Coomassie Brilliant Blue.

were examined on SDS-polyacrylamide gels and found to be 60-90% pure (Figure 3.2.1).

Section III: Characterization of mutant catalase HPiIs

Effect of Temperature on Mutant catalase HPiI Expression

The production of mutant proteins was affected by growth temperature. At 28°C, wild type HPiI yields were about the same compared to 37°C. In contrast, all mutant HPiIs exhibited maximal production at 28°C. Levels of HPiI production at 28°C ranged from 1.1 to 2.0 times that observed 37°C for mutants D197S, D197A, H392A, H392Q, H395A, H395Q, Q419A and Q419H, while double mutant D197S/ H395Q had production levels at 28°C 5.4 times those at 37°C. This effect may be due to difficulties in folding experienced by the mutant HPiIs versus wild type HPiI. Incorrectly or incompletely folded mutant HPiIs are subject to proteolytic degradation, which would be less efficient at 28°C compared to the optimum growth temperature of *E. coli* of 37°C, and chaperones would have more time to promote proper folding (Sevinc *et al.*, 1998). Mutant D197S/H395Q, the only double mutant studied in this project, appeared to have the most difficulty folding properly, with an activity per dry cell weight of only 17% of the wild type at 37°C. Single site mutants apparently had only minor folding problems (Table 3.3.1).

Table 3.3.1. Effects of growth temperature on the production of the wild type and mutant catalase HPiIs

HPiI Mutant	Catalase Activity (units/mg dry cell weight)		Activity Ratio 28°C/37°C
	37°C	28°C	
Wild Type	425 ± 51	388 ± 59	0.9
D197A	252 ± 24	394 ± 21	1.6
D197S	183 ± 15	314 ± 7	1.7
H392A	203 ± 34	429 ± 20	2.1
H392Q	395 ± 46	421 ± 30	1.1
H395A	444 ± 33	694 ± 23	1.6
H395Q	491 ± 57	745 ± 61	1.5
Q419A	652 ± 14	853 ± 17	1.3
Q419H	289 ± 26	307 ± 33	1.1
D197S/H395Q	70 ± 6	381 ± 25	5.4

Spectral Properties of Mutant Catalase HP1Is

Due to the *cis*-heme d-isomer bound to catalase HP1I, the color of purified wild type enzyme is dark green (Chiu *et al.*, 1989). Mutants D197A, D197S, H395Q, Q419H and H395A retained this coloration, but mutants D197S/H395Q and Q419A exhibited a combination of dark green and dark reddish-brown color. This is indicative of the presence of both heme d and heme b. Mutants H392A and H392Q also varied in their coloration from the wild type, with a rich brown color characteristic of protoheme in the prosthetic group.

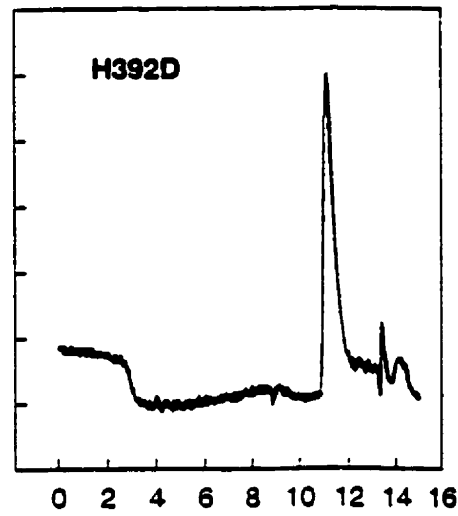
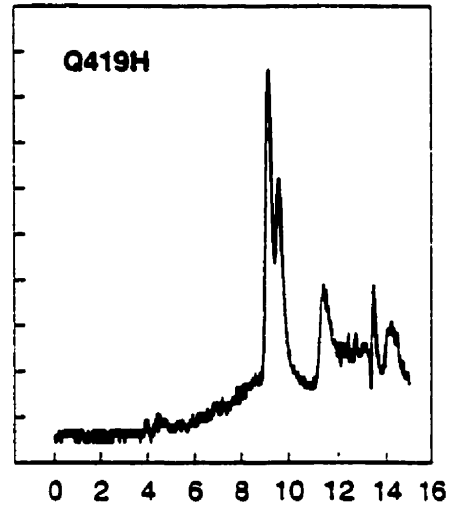
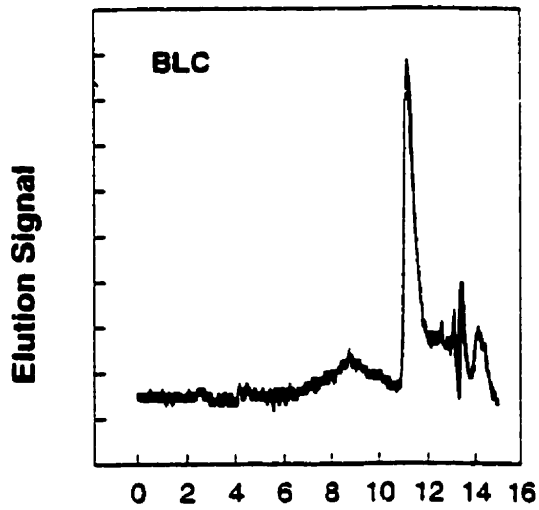
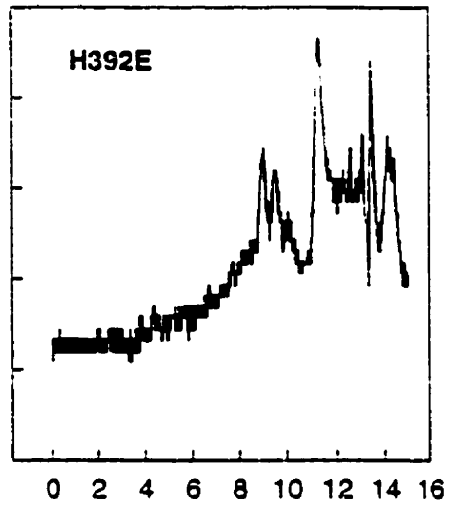
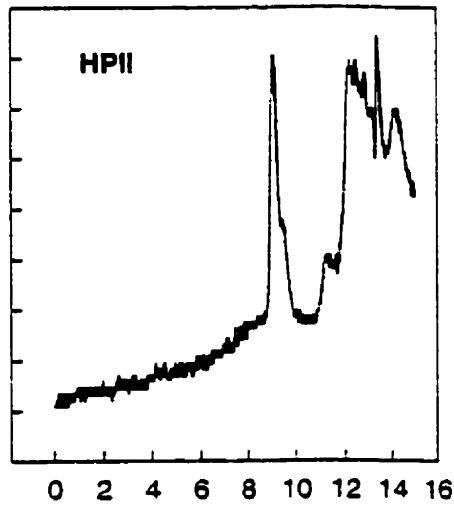
The absorbance spectra were consistent with color differences of mutants of HP1I. Heme d has two characteristic absorbance peaks at 590 and 715 nm while heme b has peaks at 535 and 630 nm. Both have a prominent Soret peak at 406 nm (Loewen and Switala, 1986). The UV and visible spectra for wild type and HP1I variants were determined (Figure 3.3.2). The spectra of the mutants Q419A and D197S/H395Q had peaks at 535, 590, 630 and 715 nm, while mutants H392A and H392Q only showed peaks at 540 and 630 nm. The remainder of the mutants exhibited absorbance peaks at 590 and 715 nm.

HPLC analysis of the extracted hemes were consistent with the spectral data obtained (Figure 3.3.1). Mutants H392A and H392Q yielded only heme b peaks, while heme from mutants D197A, D197S, H395A, H395Q and Q419H shared HPLC profiles similar to heme from the wild type enzyme, with a predominant heme d and a smaller heme b peak. In contrast, mutants Q419A and D197S/H395Q had predominant heme b peaks and smaller heme d peaks.

Table 3.3.2. Comparison of the prosthetic groups of wild type and mutant variants of HP11.

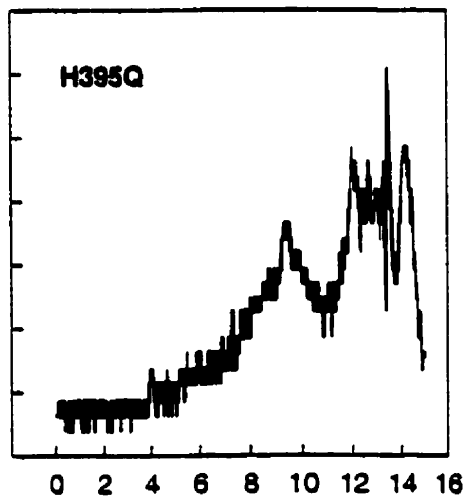
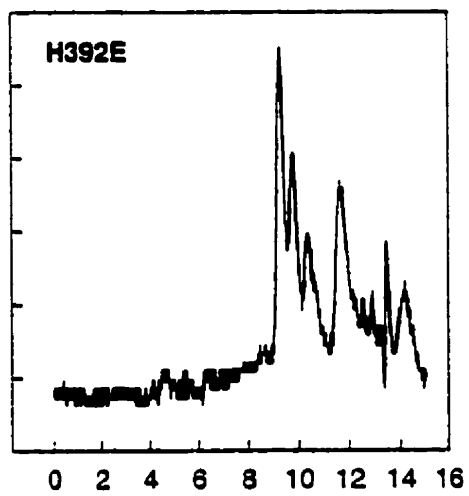
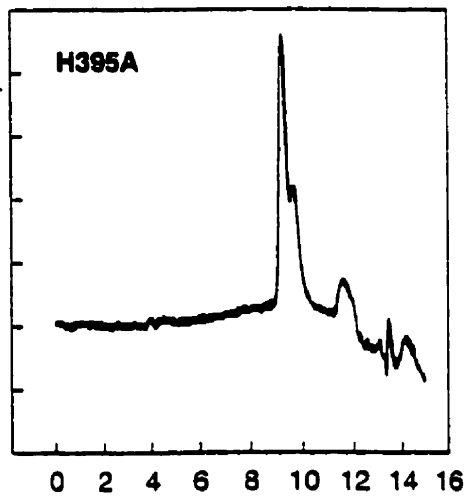
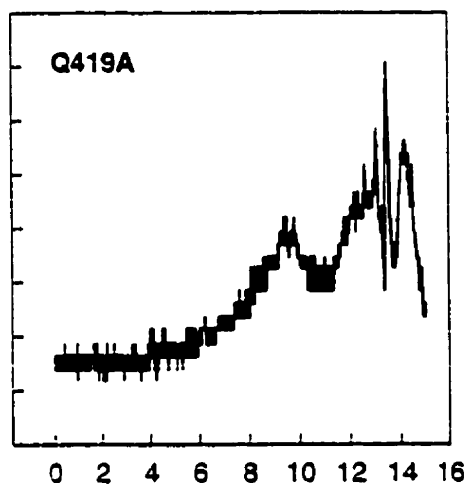
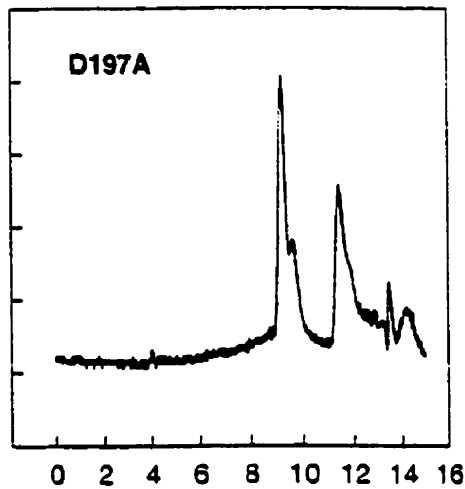
Mutant	Dominant Prosthetic Group
Wild Type	heme d
D197A	heme d
D197S	heme d
D197S/H395Q	heme b and heme d
H392A	heme b
H392Q	heme b
H395A	heme d
H395Q	heme d
Q419A	heme d and heme b
Q419H	heme d

Figure 3.3.1. Elution profiles from C18 reverse phase HPLC chromatography of heme extracted from various HPII mutants.



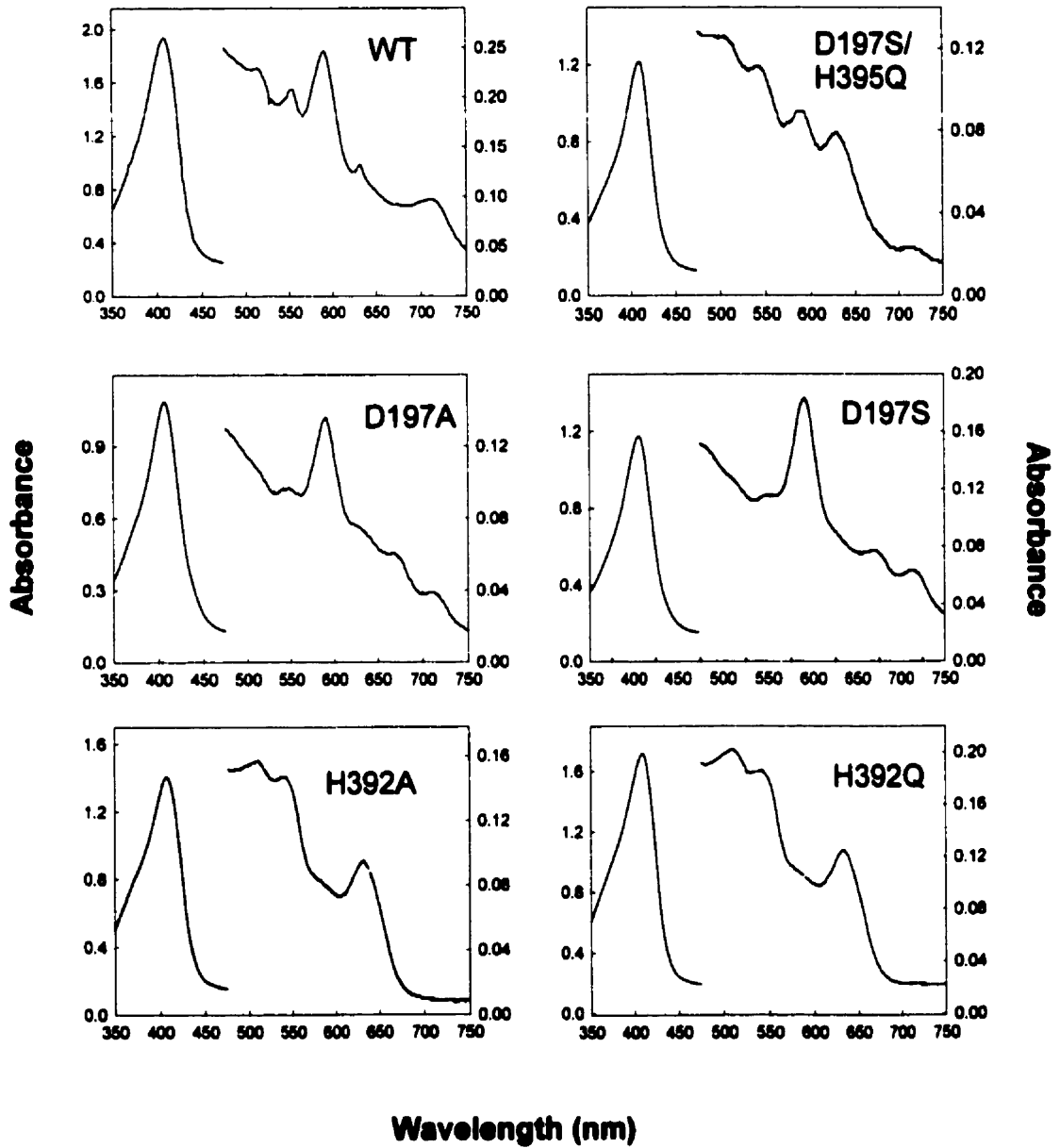
Elution Time (min)

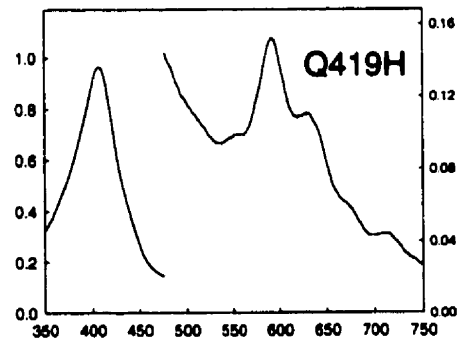
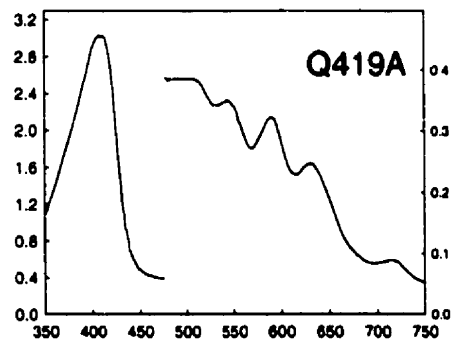
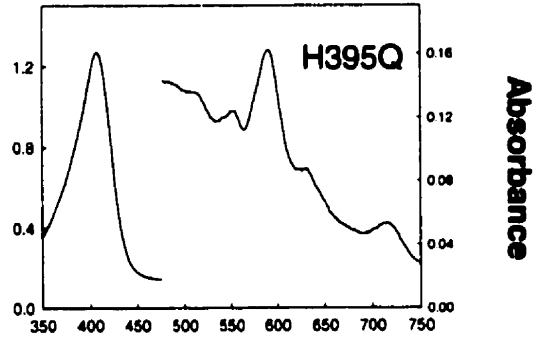
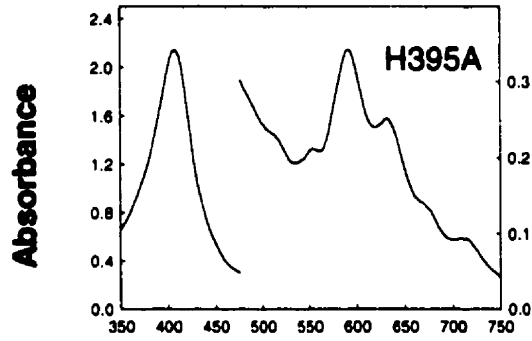
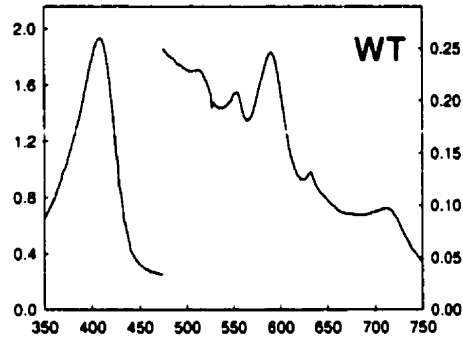
Elution Signal



Elution Time (min)

Figure 3.3.2. Absorption spectra of wild type HPII and various mutants. The left axis is for the range from 350-475 nm while the right axis is for the range from 475 to 750 nm.





Wavelength (nm)

Specific Activity and Steady-state Kinetic Properties of Mutant Catalase HP1Is

It should be mentioned that the kinetic analysis of catalases is not easy, as they do not follow the normal pattern of Michaelis-Menten saturation kinetics. Enzyme saturation with substrate cannot be obtained within a workable concentration range. This is because the 5 M hydrogen peroxide required to saturate some catalases (including HP1I) is high enough to inactivate the enzyme.

Catalase HP1I specific activities under non-substrate saturating conditions (Table 3.3.3) of mutants H392Q, H392A, H395Q and H395A ranged from 51% to 69% of wild type activity. The specific activities of HP1I mutants D197A, D197S and D197S/H395Q were not significantly different from the wild type, falling within 7% of wild type values. HP1I mutant Q419A was 21% more active than the wild type, while changing the same amino acid to histidine decreased HP1I activity 18% compared to the wild type.

The dependence of the enzyme reaction rates on substrate concentration was examined, with saturation curves generated by fitting the data with the single rectangular, two parameter equation found in the SigmaPlot software (v. 4) (Jandel, San Rafael, CA.). The apparent V_{max} (the maximal initial reaction velocity) and K_m (the substrate concentration at which the initial reaction velocity is equivalent to half the maximum initial reaction velocity) values were obtained from these curves. K_{cat} (turn over rate, $\sim 10^5 \text{ sec}^{-1}$) was calculated in order to give the number of substrate molecules converted to product per unit time by each active site of the enzyme at saturating substrate concentrations (the turnover

number). This in turn was used to interpret the structural effects of amino acid changes in HP11 mutants in comparison to wild type HP11. The influence of H_2O_2 concentration on initial enzyme velocities rate (V_i) of the mutant and wild-type HP11s revealed similar kinetic responses, with much lower V_i at low $[H_2O_2]$ and much less sensitivity to higher $[H_2O_2]$ compared to BLC (BLC data from Sevinc S. M. *et al.*, 1999 not shown here). As shown in Table 3.3.3, the turnover rate for most mutants fell within the same range as that for the wild type enzyme when standard deviations are considered, except for mutants H395A, D197A and H392A. Mutants H395A and D197A exhibited a small increase, while H392A showed a small decrease in turnover rate when compared to wild type HP11.

The observed differences in activity and turnover rates of mutant HP11s when compared with wild type HP11 may be correlated with differences in the heme pocket, the substrate entry channels and product exhaust channel. For example, mutants H392A and H392Q which have heme b as the prosthetic group also exhibit a 40-50% decrease in specific activity compared to wild type HP11.

Three channels have been found within HP11 protein (Bravo, J., *et al.*, 1999). Two are close to the distal side heme pocket of each subunit, suggesting separate inlet and exhaust functions. The third channel reaches the heme proximal side where all mutants studied in this project were located, and is thought to provide access for the substrate needed to catalyze the heme modification and His392-Tyr415 bond formation. This channel is still not as clearly defined as the first two channels, and until now has presented some discontinuities. However, changing H395 still slightly affects the specific activity

of the enzyme and since the prosthetic group is not different, there is the implication that a long range alteration of tertiary structure may play a role.

Effect of High Temperature on mutant HP11 Catalase Activities

HP11 catalase is a very stable enzyme exhibiting high activity during incubation at 65°C. Wild type HP11 retained full specific activity (Figure 3.3.4) with an approximate 20% increase in specific activity after an hour at 65°C. The mutants of HP11 exhibited some thermal instability. Under the same conditions, mutants D197A and D197S/H395Q lost around 45% of their specific activity, while mutants H395Q and Q419A showed a slight decrease in specific activity of around 15-20%. Mutants H392A and H392Q were the most different from wild type HP11, losing about 40% of their activity after 10 minutes at 65°C and about 65-70% of their activity after incubation at 65°C for one hour.

All mutants showed much higher stability compared to BLC, which is completely inactivated within 30 minutes at 64°C, and HP1 which is completely inactivated within 15 minutes at 58°C (Switala, J. *et al.*, 1999). The differences observed between HP11, BLC and HP1 can be rationalized in terms of a number of unusual features characteristic of HP11. One distinct feature of HP11 is the 90 N-terminal residue overlap between subunits. Another feature is the unusual covalent bond between His392 and Tyr415. Mutant H392A and H392Q, which prevent the formation of this bond, showed greater sensitivity to high temperature compared to wild type HP11. This data supports the idea that the extra covalent bond could help stabilize the enzyme. This contradicts the conclusions obtained from the study of two other mutants of HP11, His128Ala and Asn201His. These

showed that His-Tyr bond is not important in the maintenance of enhanced resistance to heat denaturation (Switala, J. *et al.*, 1999). Further studies will be necessary to rationalize these conflicting results.

Effect of Cyanide and Azide on Mutant HPII Catalase Activities

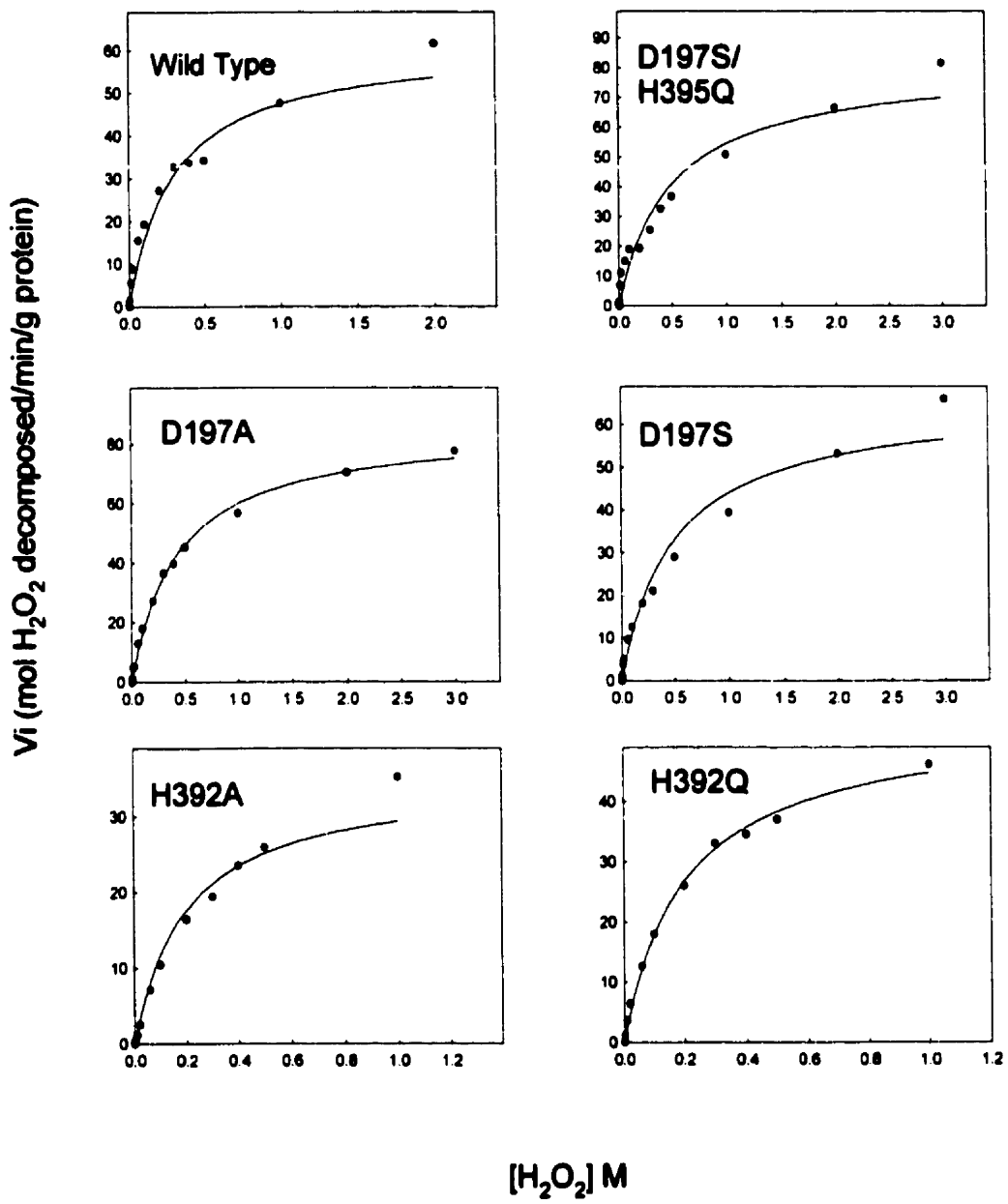
Both cyanide and azide have been reported to reversibly inhibit catalase by binding to the heme iron (Beyer and Fridovich, 1988). Both inhibitors alter HPII's visible absorbance spectrum, including a red shift in both the Soret band and A_{590} peak by cyanide and an increase in the A_{630} peak by azide if heme d is the prosthetic group (Figure 3.3.7). In contrast, addition of cyanide to HPII with a heme b prosthetic group results in a red shift of the Soret band, as well as the appearance of an absorbance peak at 545 nm with a shoulder at 590 nm, and a significant decrease in the 630 nm peak. No changes are caused by binding azide to heme b. Based on the heme present, the absorbance changes observed were as expected. For example, D197S/Q395H and Q419A appeared to be a mixture of heme b and heme d.

Both wild type and mutant HPIIs were found to require much higher concentrations of azide (Figure 3.3.5) than cyanide (Figure 3.3.6) to inhibit their activity by 50%. Some mutants had a slight increase in sensitivity toward azide. This might possibly be explained by the removal of important amino acid side chains and the disruption of H395-H392, D197-H395, Q419-D417 and Q419-S421 hydrogen bonds. These consequently loosen the tightly folded enzyme and allow the CN^- and N_3^-

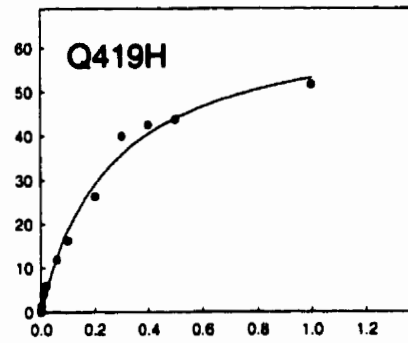
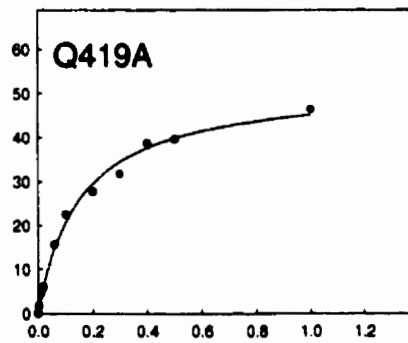
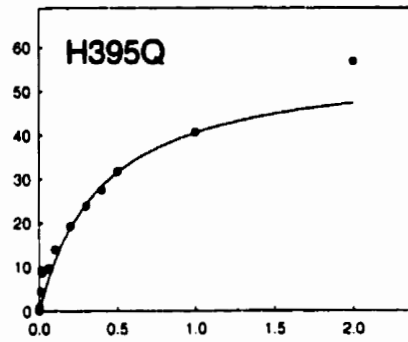
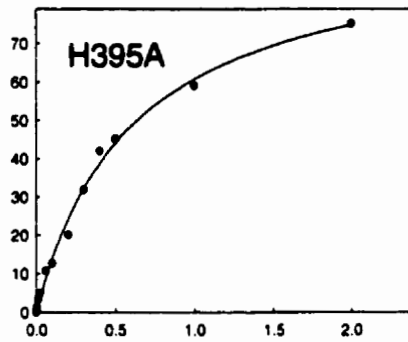
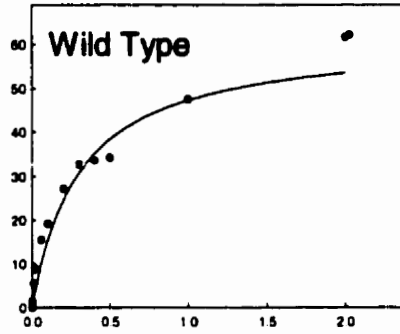
Table 3.3.3. Specific activities and Kinetic parameter of the mutant and wild type HPII catalases

Enzyme	Specific Activity (Units/mg)	K_m (mM)	V_{max} (mol/min/g)	K_{cat} (x10⁵ sec⁻¹)
D197A	14,354	432.6	85.8	1.19
D197S	14,721	500	66	0.93
D197S/H395Q	15,473	500	81.5	1.13
H392A	8,875	200	35.2	0.49
H392Q	7,368	202	53.8	0.75
H395A	9,821	604.7	97.5	1.36
H395Q	9,224	400	56.7	0.79
Q419A	17,361	151	52	0.72
Q419H	11,703	261.8	67.1	0.93
Wild Type	14,322	300	61.6	0.85

Figure 3.3.3. Comparison of the effect of hydrogen peroxide concentrations on the initial velocities (V_i) of wild type HPII and various mutants.



V_i (mol H_2O_2 decomposed/ min/g protein)



[H₂O₂] M

easier access to the catalytic site. The different observed effects of mutations upon cyanide and azide sensitivity may be explained in part by the differences in the sizes of these inhibitors. The molecular weights of cyanide, hydrogen peroxide and azide are 26 Da, 34 Da and 42 Da respectively. The similar degree of sensitivity of wild type HP11 and mutants D197S, H395A, H395Q and Q419H to cyanide supports the hypothesis that the heme channel of HP11 has evolved to accommodate molecules the size of its substrate, H₂O₂ with even small changes in substrate size (such as to azide) affecting accessibility. It is known that the inlet and exhaust channels are both located on the distal side of the prosthetic group. The way in which the mutants of H395, Q419 and D197 (all located on the proximal side of the prosthetic group) can affect the rate at which substrate accesses the heme and whether or not the proposed third channel of HP11 is involved in this effect requires further study. In addition to the rate of inhibitor entry and exit from the catalytic site, differences in the type of prosthetic group, inhibitor binding affinity and dissociation rate in the mutant and wild type HP11s may also help to account for the phenotypes observed. Friend *et al.* (1980) found that every acidic or basic group in the sperm whale metmyoglobin (which also contains heme b as its prosthetic group) can contribute to the binding affinity of the azide anion. Three ionizable groups in metmyoglobin have been found to influence the rate of azide and cyanide association (Lin, J. *et al.*, 1999). These are the distal His64, heme propionate and His97 in the heme proximal pocket. The kinetics of the formation and dissociation of the mutant HP11/inhibitor complex must be studied in order to give a better understanding of the

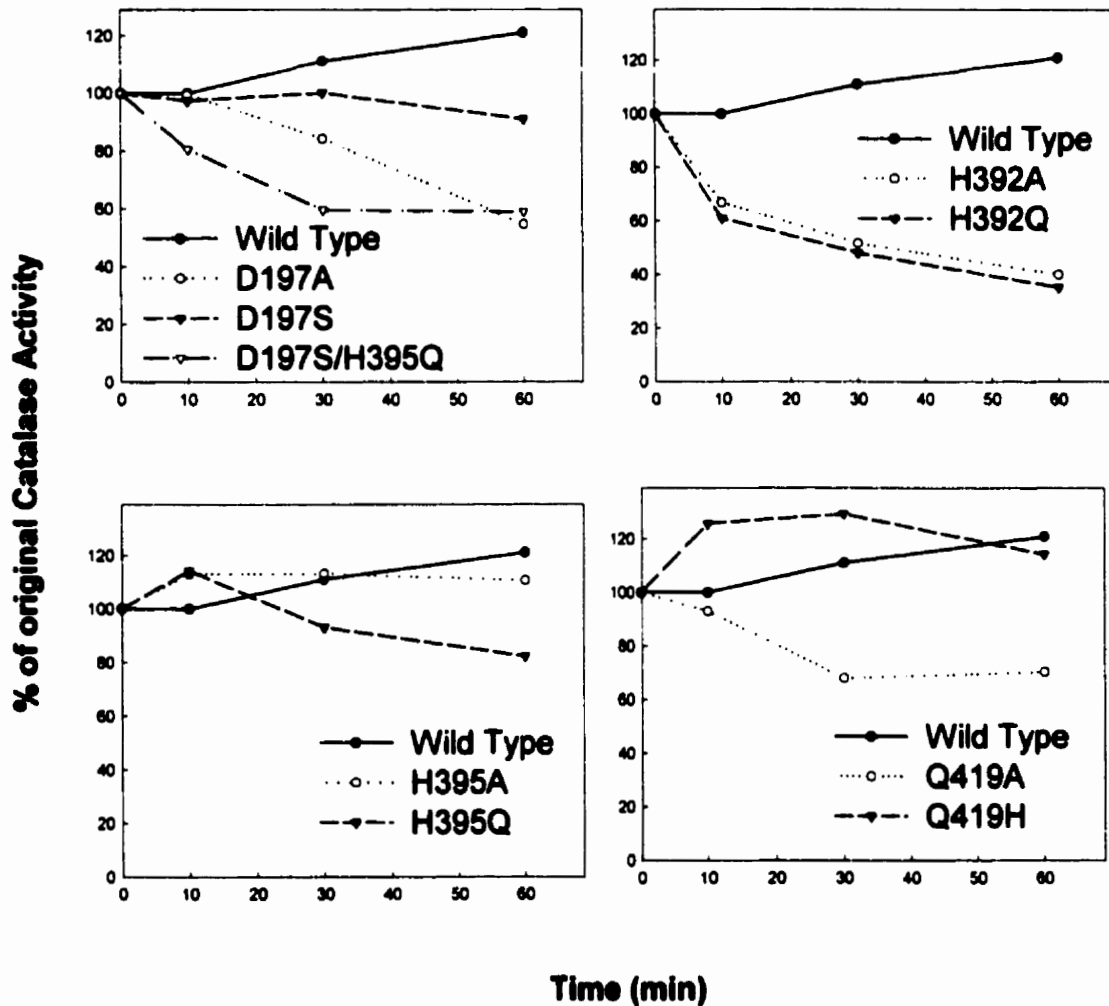


Figure 3.3.4. Determination of the activity of mutant and wild type HP11 catalases during incubation at 65°C. Each of the enzymes was incubated at 65°C in 50 mM potassium phosphate buffer (pH 7.0), and aliquots were removed at various times and assayed. Data are expressed as a percentage of original activity.

mechanism(s) involved in the alteration of the cyanide and azide inhibition in the mutant HPiIs studied here.

Effect of NH_2OH , CH_3ONH_2 , $\text{C}_2\text{H}_5\text{ONH}_2$ on Mutant HPiI Catalase

Hydroxylamine has been reported to react with compound I of catalase to form nitric oxide (Marcocci *et al.*, 1994), which reversibly reacts with heme to cause inhibition of the enzyme (Doyle *et al.*, 1981; Brown, 1995) by structurally changing the heme proximal pocket environment (Zhao, Y., *et al.*, 1998). The inhibitory effects of hydroxylamine (H_2NOH) and its derivatives O-methylhydroxylamine (NH_2OCH_3) and O-ethylhydroxylamine ($\text{NH}_2\text{OC}_2\text{H}_5$) were studied. Inhibition by hydroxylamine was effective at nM concentrations whereas mM concentrations of methylhydroxylamine and ethylhydroxylamine were required to achieve the same degree of inhibition. Similar to the effects of cyanide and azide, this is likely due to the size differences of the inhibitors. Generally speaking, larger inhibitors have more difficulty in accessing the active site, therefore requiring higher concentrations to achieve the same level of inhibition.

Mutants H392A and H392Q exhibited the most significant differences from wild type HPiI (Figures 3.3.8, 3.3.9, 3.3.10 and 3.3.11, Table 3.3.4). Consistent with the inhibition results for cyanide and azide, wild type HPiI showed much greater sensitivity to H_2NOH and NH_2OCH_3 than these mutant HPiIs, but had similar sensitivity to $\text{NH}_2\text{OC}_2\text{H}_5$. This implies that the inhibitors have more difficulty accessing the active site of the mutants H392A and H392Q

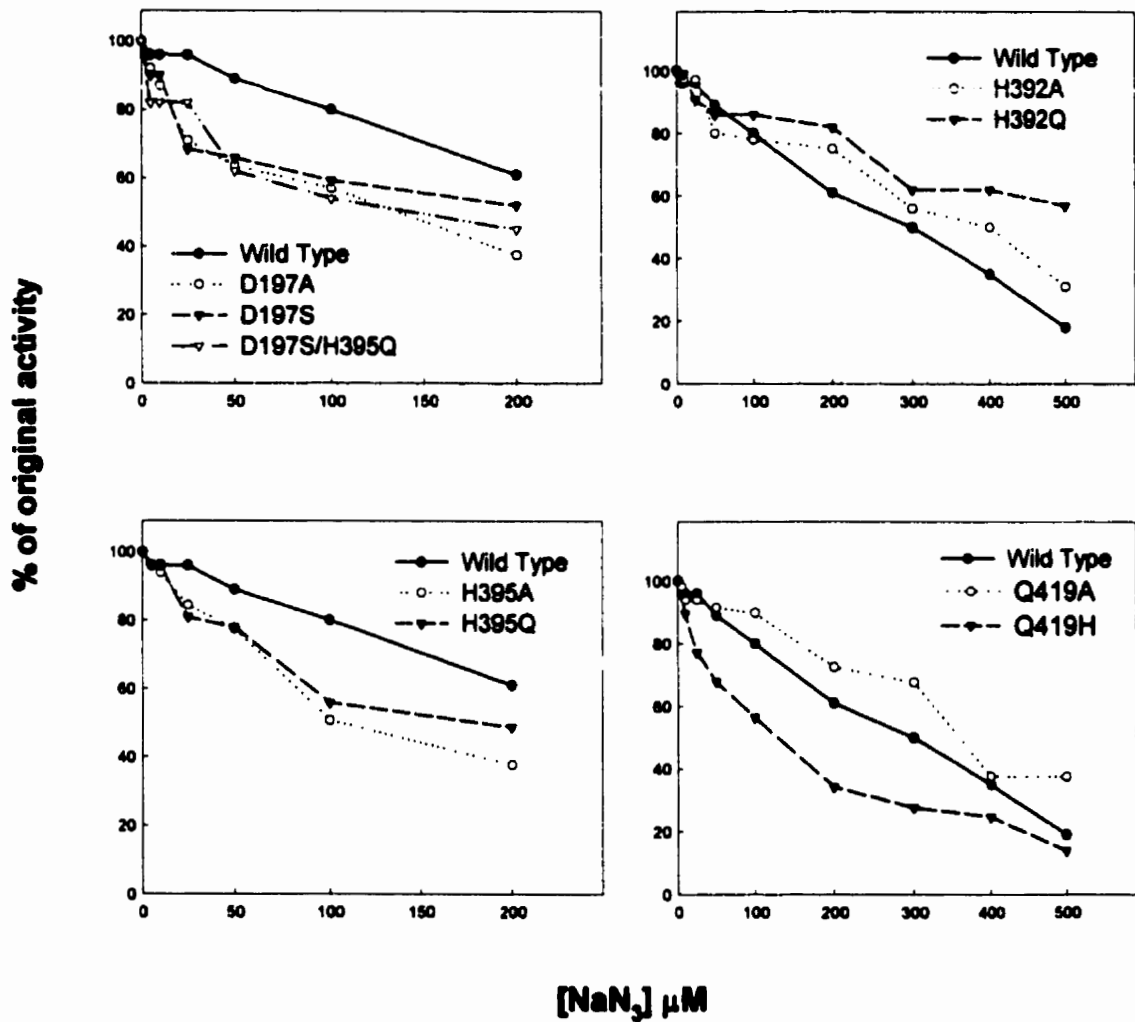


Figure 3.3.5. Comparison of the effects of sodium azide on mutant and wild type HPII catalases activities.

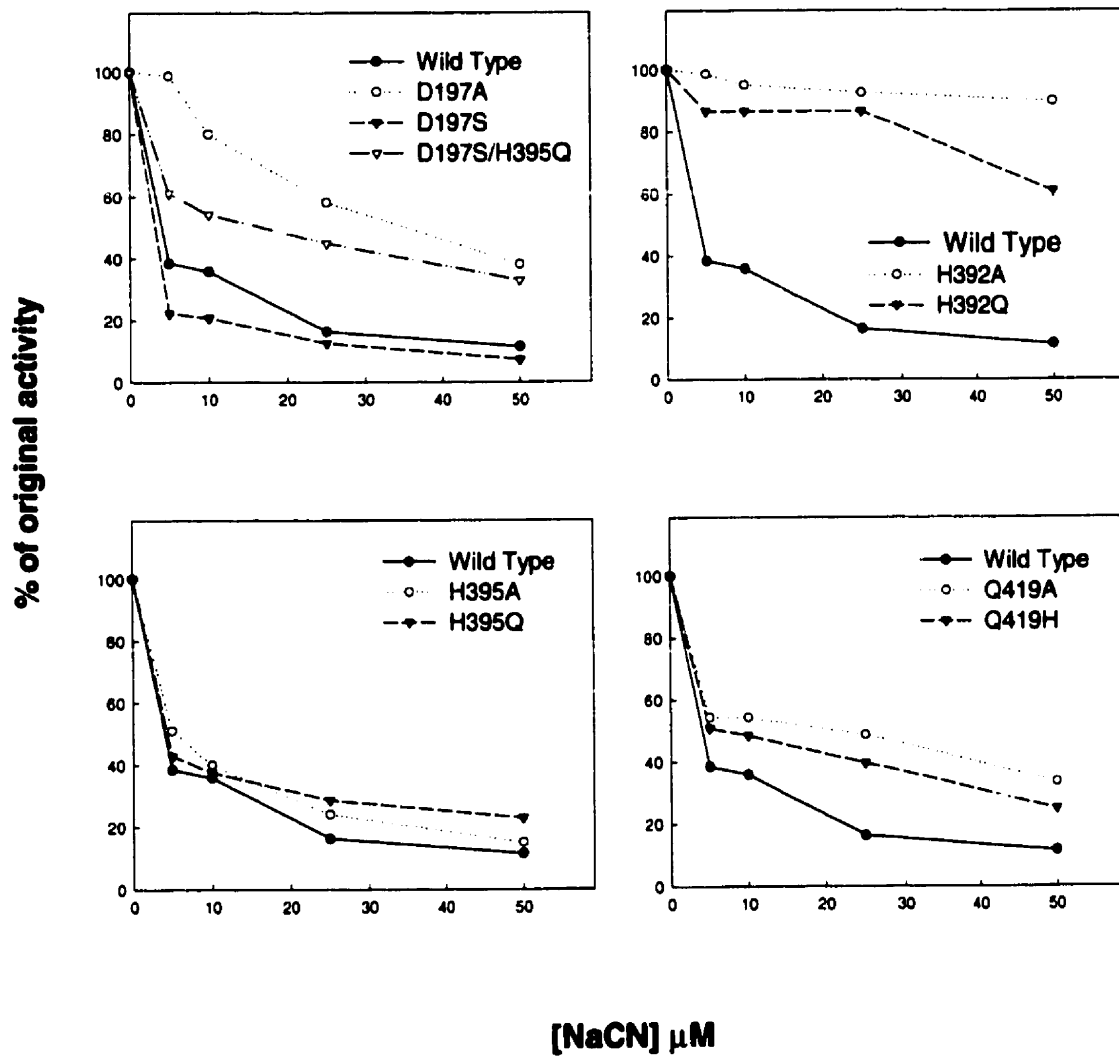
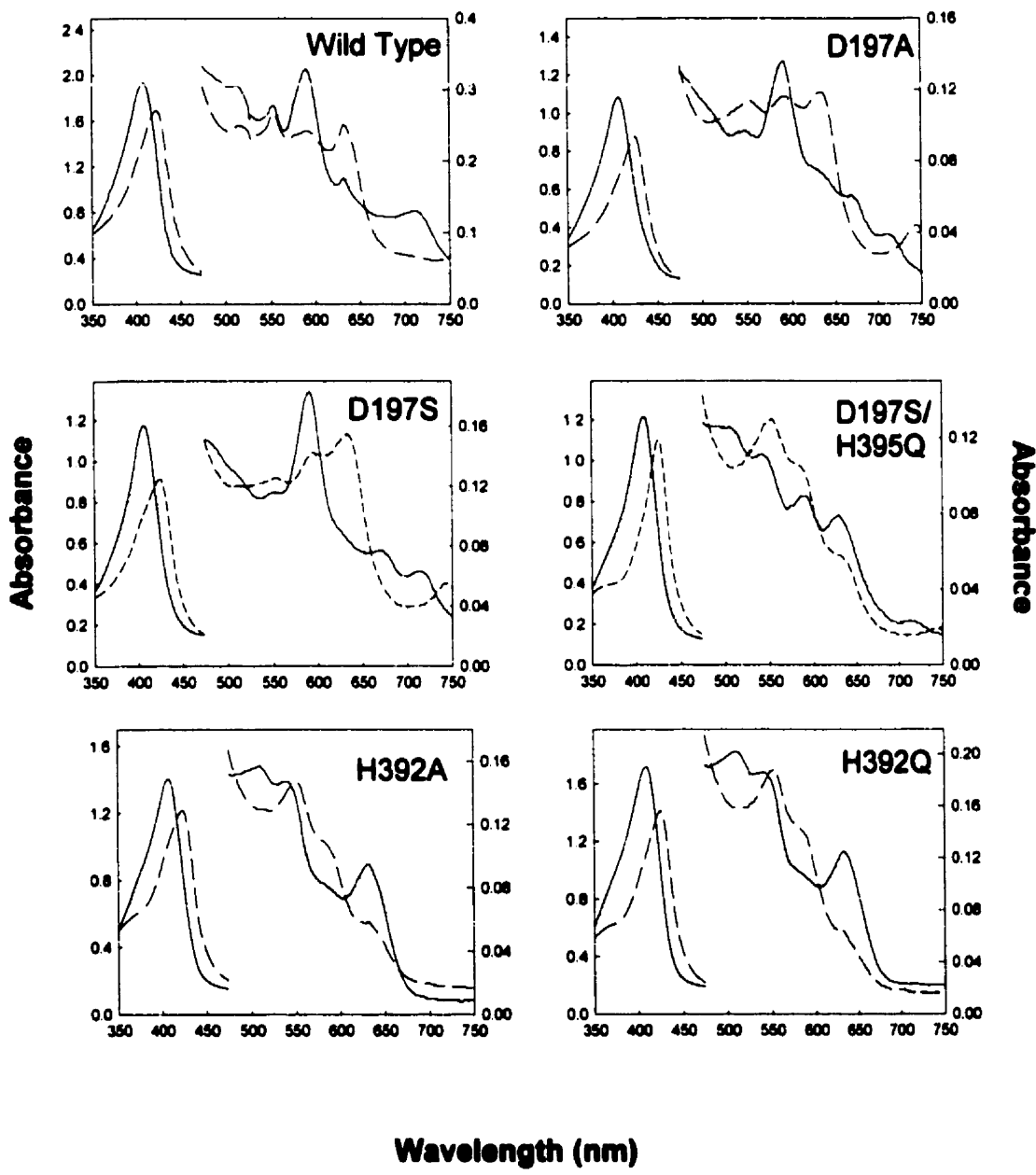
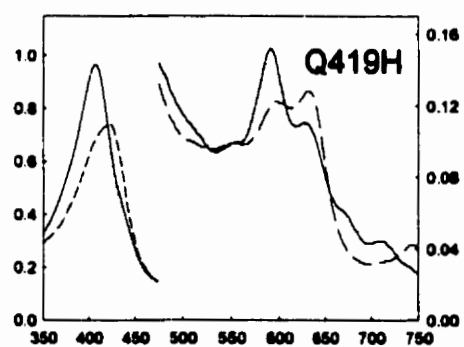
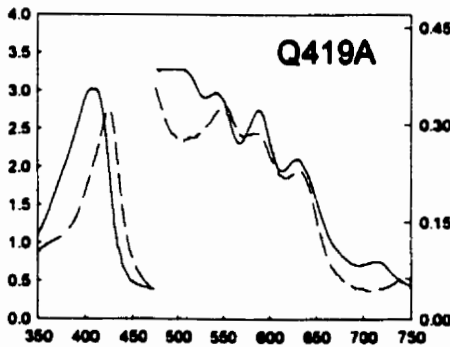
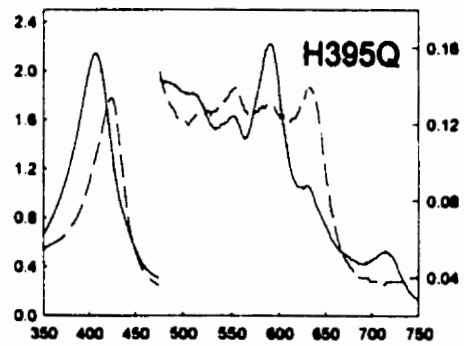
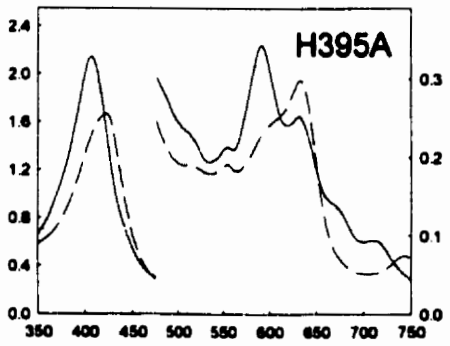
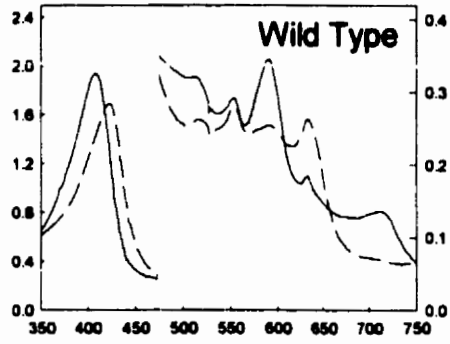


Figure 3.3.6. Comparison of the effects of sodium cyanide on mutant and wild type HPII catalases activities.

Figure 3.3.7. Absorption spectra of mutant and wild type HPII catalases in the presence and absence (_____) of NaCN and NaN₃. Each enzyme was incubated with 0.5mM NaCN(-----) and 1 mM NaN₃(.....) at room temperature for 15 min prior to spectral analysis. The left axis is for the range from 350 to 475nm while the right axis is for the range from 475 to 750 nm.





Absorbance

Wavelength (nm)

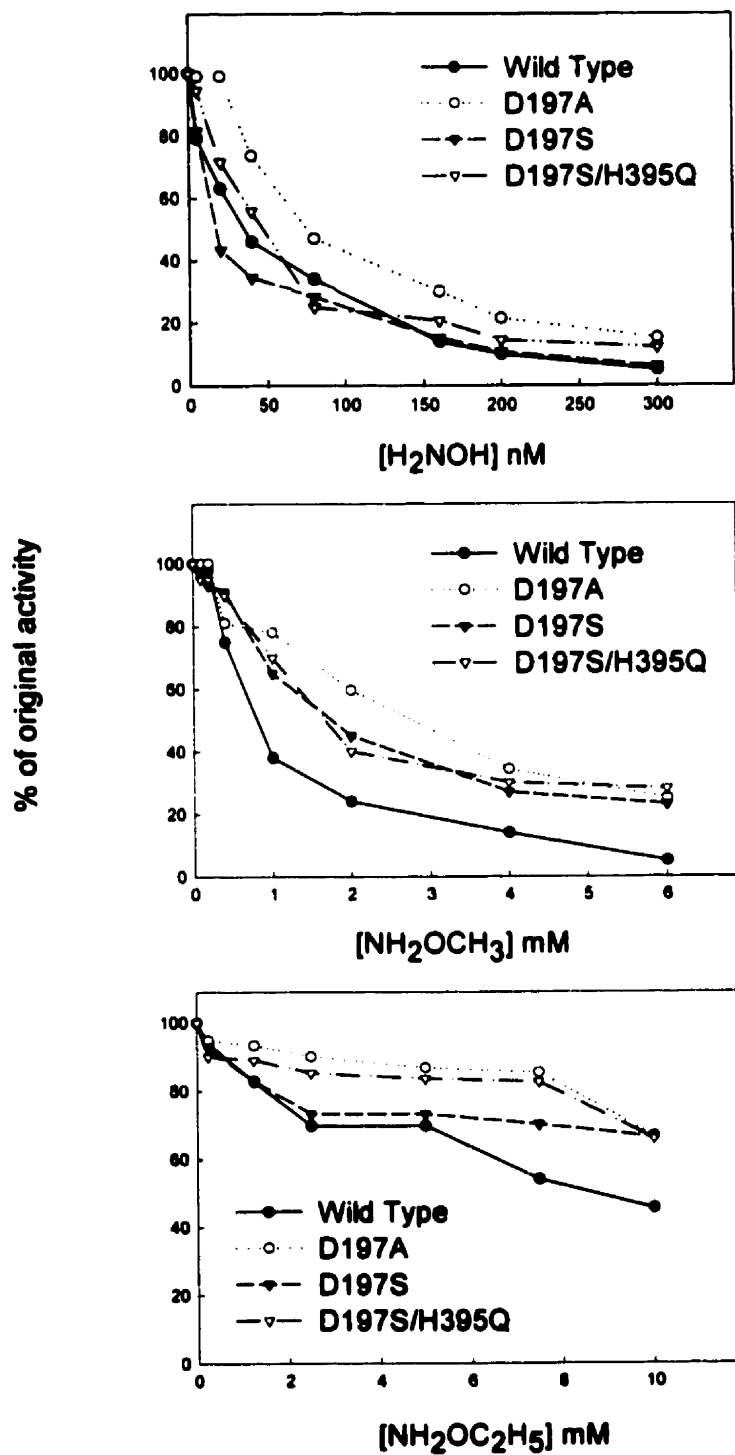


Figure 3.3.8 Comparison of the effects of various hydroxylamine derivatives on mutant D197A, D197S, D197S/H395Q and wild type HPII catalases activities.

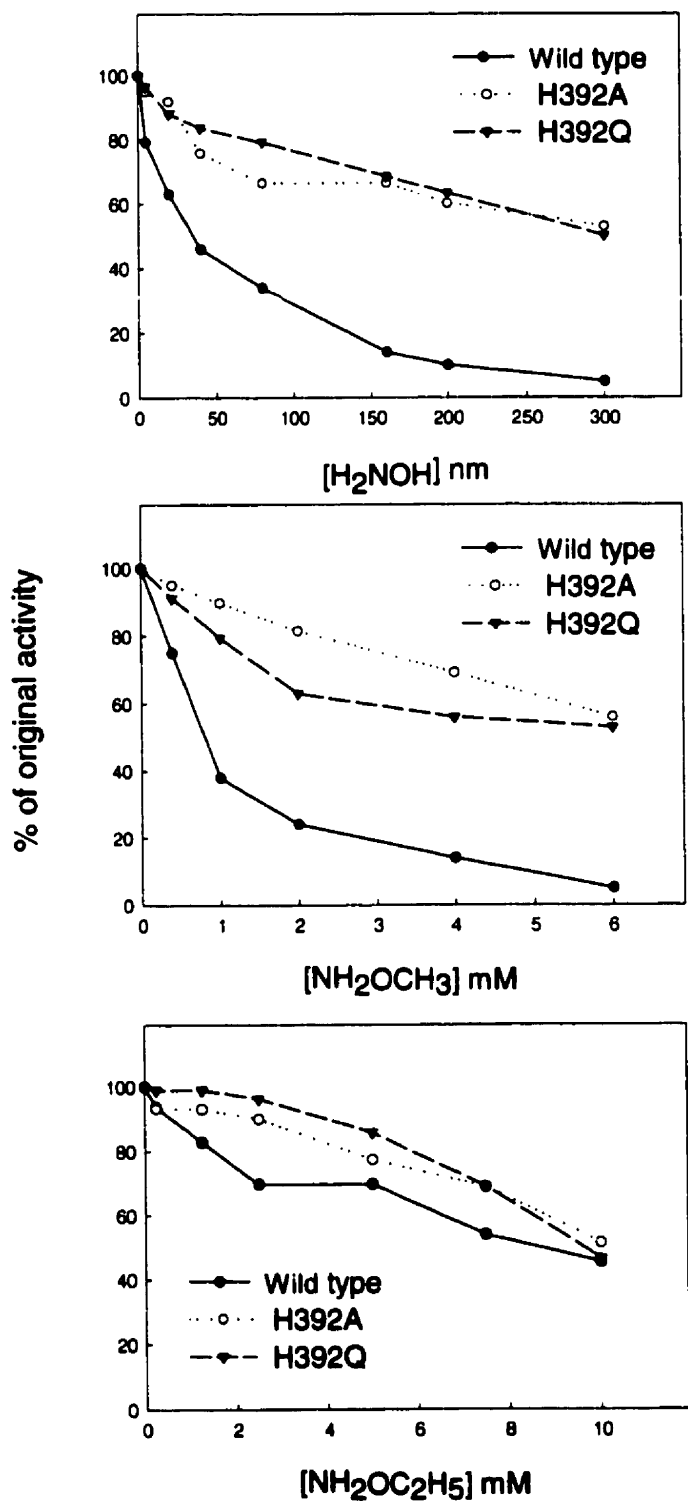


Figure 3.3.9. Comparison of the effects of various hydroxylamine derivatives on mutant H392A, H392Q and wild type HPII catalases activities.

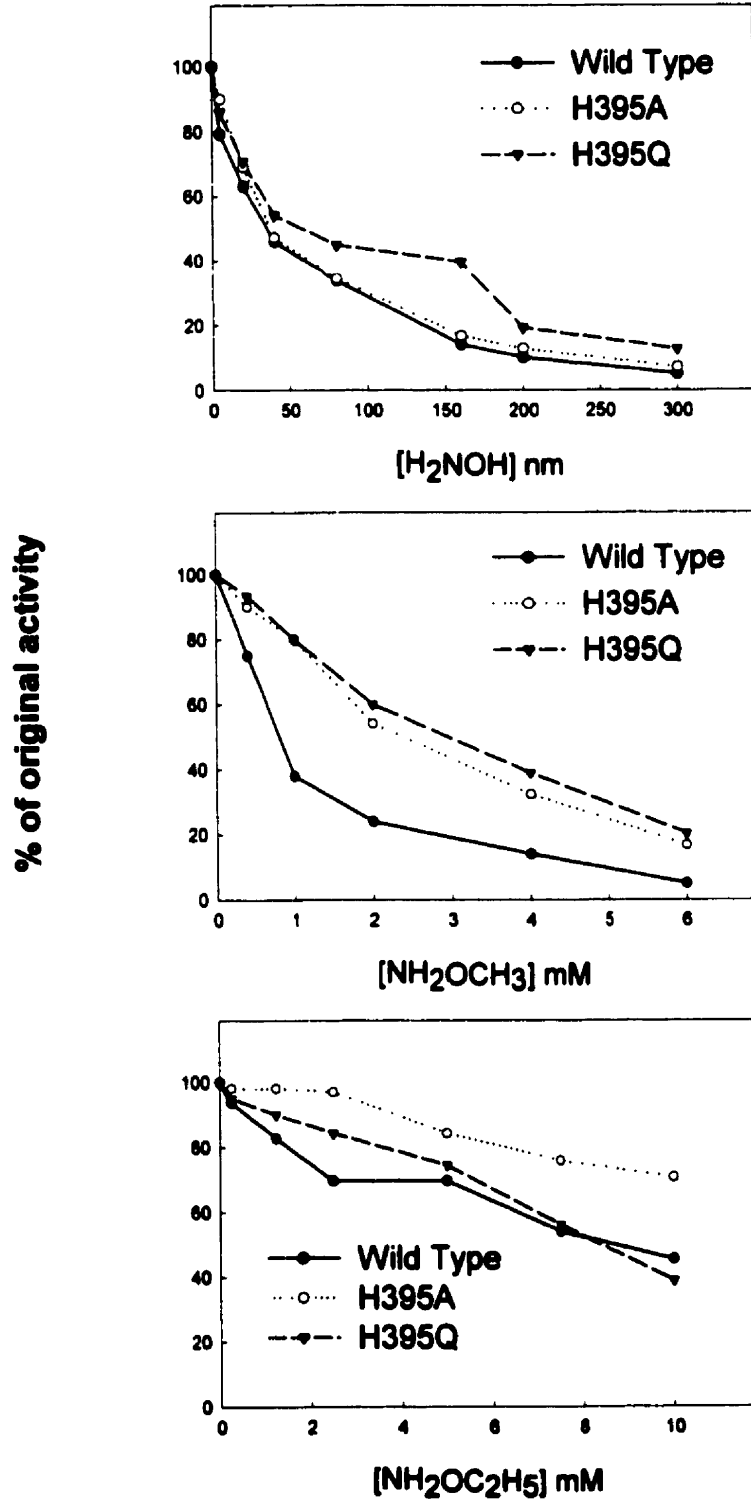


Figure 3.3.10. Comparison of the effects of various hydroxylamine derivatives on mutant H395A, H395Q and wild type HPII catalases activities

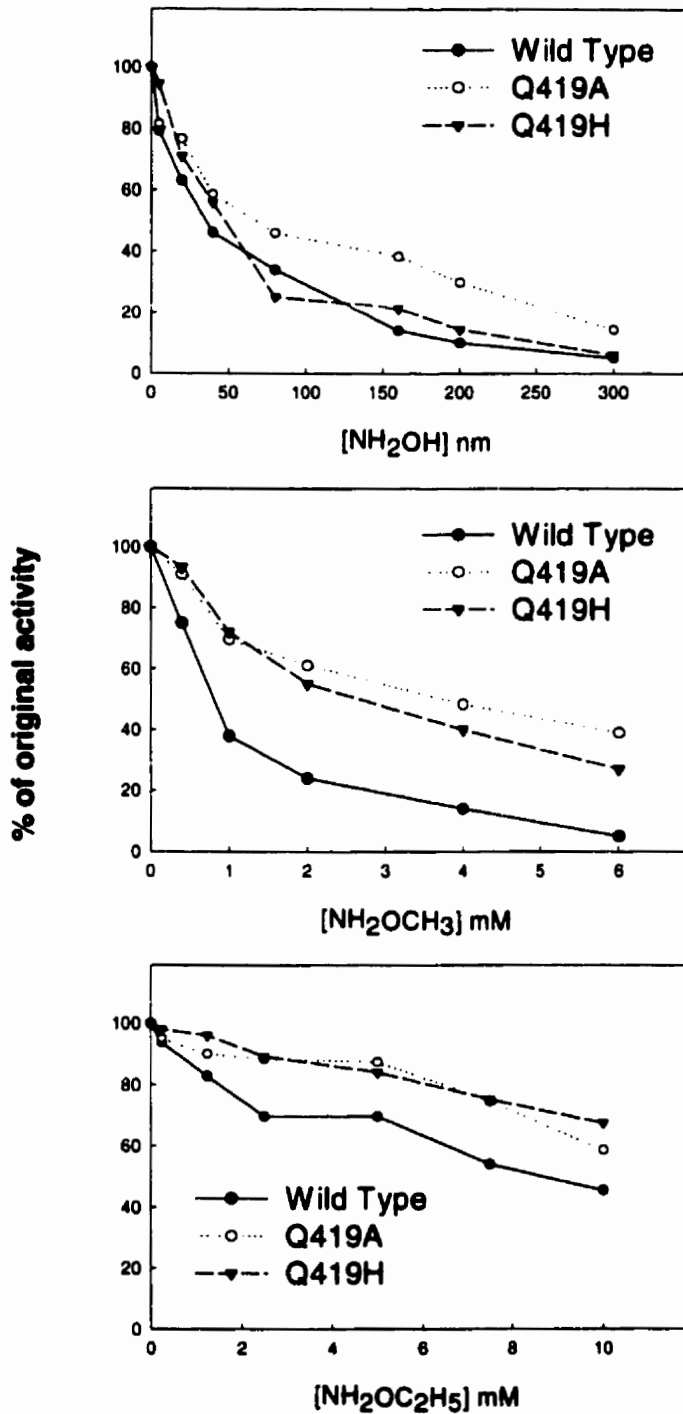


Figure 3.3.11 Comparison of the effects of various hydroxylamine derivatives on mutant Q419A, Q419H and wild type HPII catalases activities.

Table 3.3.4. Determination of the 50% inhibitory concentrations of nine mutant HPII catalases compared with wild type HPII enzyme.

Enzyme	$\mu\text{mol/l}$ needed for 50% inhibition				
	NaCN	NaN ₃	NH ₂ OH	NH ₂ OCH ₃	NH ₂ OC ₂ H ₅
D197A	35.2	135	0.076	2750	12200
D197S	3.1	232	0.018	1720	19600
D197S/H395Q	17	144	0.047	1680	12200
H392A	250	395	0.3	6800	10000
H392Q	61	620	0.33	8000	9550
H395A	5.3	105	0.0375	2350	20000
H395Q	4.5	180	0.055	2900	8400
Q419A	21.5	358	0.048	3730	11400
Q419H	6.7	128	0.066	2670	16000
Wild Type	4.2	300	0.035	800	8550

compared to wild type HP11, but if the inhibitor is big enough there are no significant differences its ability to access the active site. In addition to mutants H392A and H392Q, wild type HP11 also showed more sensitivity to these inhibitors than the other mutants. The effects are relatively small.

Section III: Summary

In this project, the effects of the mutation of residues involved in the formation of the His392-Tyr415 covalent bond on the proximal side of the prosthetic heme group of HP11 were studied.

Changing H392 to alanine or glutamine caused similar phenotypic effects, with the His-Tyr bond not being formed and heme b to heme d conversion being inhibited. These results support the mechanistic relationship between the autocatalytic conversion of heme b to heme d and the formation of the His392-Tyr415 bond proposed by Bravo *et al.* (1997a). With heme b as the prosthetic group, mutant H392A and H392Q exhibit greater sensitivity to high temperature as well as slightly lower specific activities and turnover rates compared to wild type HP11. Higher concentrations of the inhibitors NaCN, NaN₃, NH₂OH, NH₂OCH₃ and NH₂OC₂H₅ were required to cause 50% inhibition of mutant HP11 specific activity compared to the wild type.

H395 forms hydrogen bonds with H392 and D197. The mechanistic hypothesis coupling His-Tyr bond formation and heme conversion (Bravo *et al.*, 1997a) predicts that H395 and D197 are involved in the extraction of a proton from the N_ε of His392 to facilitate the formation of the His-Tyr bond. In contrast to the H392 alterations which prevented both His-Tyr bond formation and heme

conversion, H395A, H395Q, D197A, D197S and D197S/H395Q all had no effect on either reaction, implying that another factor is involved with proton extraction. No significantly different phenotypic properties were observed in these mutant HP1Is, except that the double mutant showed the most difficulty in folding properly when compared to other mutants. The double mutant also exhibited a higher heme b content than the wild type, which was not seen in individual site mutants. It would appear that the D197-H395-H392 hydrogen bond is used to form the His-Tyr bond, but in the absence of D197, H395 can use other residues as substitutes. D197 can work in a similar way in the absence of H395. This implies that in addition to the D197-H395-H392 proton extraction pathway, alternative pathways may also exist, suggesting that the mechanism involved in the His-Tyr bond formation is not as simple as has been proposed.

Q419 also forms hydrogen bonds with heme d and may help to orient H_2O_2 on the proximal side of heme d, for His-Tyr bond formation. The Q419H variant exhibited the same spectral properties as the wild type, whereas Q419A was shown to have a mixture of heme b and heme d, suggesting that the Q419 side chain does have a role in His-Tyr bond formation and heme conversion.

4. REFERENCES

- Allgöcd, G.S., and Perry, J.J. 1986. Characterization of a manganese-containing catalase from the obligate thermophile *Thermoleophilium album*. *J. Bacteriol.* 168: 563-567
- Altuvia, S., Aliron, M., Huisman, G., Kolter, R., and Storz, G. 1994. The *dps* promoter is activated by OxyR during growth and by IHF and σ^S in stationary phase. *Molec. Microbiol.* 13:265-272
- Arms, B.N. 1983. Dietary carcinogens and anticarcinogens. *Science* 221:1256-1264
- Barth, M., Marschall, C., Muffler, A., Fischer, D., and Hengge-Aronis, R. 1995. Role for the histone-like protein H-NS in growth phase-dependent and osmotic regulation of σ^S and many σ^S -dependent genes in *Escherichia coli*. *J. Bacteriol.* 177:3455-3464
- Bearson, S.M.D. Benjamin Jr., W., Swords, W.E., and Foster, J.W. 1996. Acid shock induction of RpoS is mediated by the mouse virulence gene *mviA* of *Salmonella typhimurium*. *J. Bacteriol.* 178:2572-2579.
- Bergdoll, M., Remy, M.-H. Cagon, C., Masson, J.M., and Dumas, P. 1997. Proline-dependent oligomerization with arm exchange. *Structure.* 5:391-401
- Berthet, S., Nykyri, L.M., Bravo, J., Mate, M.J., Berthet-Colominas, C., Alzari, P.M., Koller, F., Fita, I., 1997. Crystallization and preliminary structural analysis of catalase A from *Saccharomyces cerevisiae*. *Prot. Sci.* 6(2): 481-483
- Beyer W. F. and I. Fridovich. 1988. Catalases: with and without heme. In *Oxygen Radicals in biology and Medicine*, M.G. Simic, K.A. Taylor, J.F. Ward and C. von Sonntag (eds.), Plenum Press, New York
- Bosshard, H.R., Anni, H. and Yonetani, T. 1991. Yeast cytochrome c peroxidase. In: *Peroxidases in Chemistry and Biology*, Everse, J. et al., eds. 11:51-84. CRC Press, Boca Raton
- Bravo, J., Fita, I., Ferrer, J.C., Ens, W., Hillar A., Switala, Jacek. and P.C. Loewen, 1997a. Identification of a novel bond between a histidine and the essential tyrosine in catalase HPII of *Escherichia coli*. *Protein science.* 6:1016-1023
- Bravo, J., Fita, I., Gouet, P., Jouve, H.-m., Melik-Adamyanyan, W., and Murshudov, G.N., 1997b. In scandalios, J. (ed), *oxidative stress and the molecular Biology of Antioxidant Defenses*. Cold Spring Harbor laboratory Press, Cold Spring Harbor, NY, 407-445

- Bravo, J., Mate, J.M., Schneider, T., Switala, J., Wilson, P., Loewen, P., Fita, I. 1999. Structure of catalase HP11 from *Escherichia coli* at 1.9 Å resolution. *Proteins*. 34:155-166
- Bravo, J., N. Verdaguer, J.Romo, C.Betzel, J.Switala, P.C.Loewen, and I.Fita. 1995. Crystal structure of catalase HP11 from *Escherichia coli*. *Structure* 3:491-502
- Brawn K., I.Fridovich. 1981. Strand scission by enzymatically generated oxygen radicals. *Arch. Biochem. Biophys.* 206:414-419
- Brodie, A.E., and D.J. Reed. 1987. Reversible oxidation of glyceraldehyde-3-phosphate dehydrogenase thiols in human lung carcinoma cells by hydrogen peroxide. *Biochem. Biophys. Res. Com.* 148:120-125
- Brot, N., L. Weissbach, . Werth and H. Weissbach. 1981. Enzymatic reduction of protein-bound methionine sulfoxide. *Proc. Natl. Acad. Sci. USA.* 78:2155-2158
- Brown G. C. 1995. Reversible binding and inhibition of catalase by nitric oxide. *Eur. J. Biochem.* 232: 188-191.
- Catalano, C.E., Cheo, Y.S., and Ortiz de Montellano, P.R. 1989. Reactions of the protein radical in peroxide-treated myoglobin. Formation of a heme-protein cross-link. *J. Biol. Chem.* 264:10534-10541
- Cerutti P.A. 1985. Prooxidant states and tumour production. . 227:375-381
- Chance, B. 1954. Enzyme mechanisms in living cells. In a symposium on the mechanism of Enzyme action. pp. 399-460. W.D. McElroy and B. Glass (eds.) The John Hopkins Press, Baltimore.
- Chance, B., H. Sies and a. Boveris. 1979. Hydroperoxide metabolism in mammalian organs, *Physiol. rev.* 59:527-605
- Chehesbro, W. 1988. The domains of slow bacterial growth. *Can. J. Microbiol.* 34:427-435.
- Chiu, J.T., P.C. Loewen, J.Switala, R.B. Gennis and R. Timkovich. 1989. Proposed structure for the prosthetic group of the catalase HP11 from *Escherichia coli*. *J. Am. Chem. Soc.* 111:7046-7050
- Chuang, W-J., and Van Wart, H.E. 1992. Resonance raman spectra of horseradish peroxidase and bovine liver catalase compound I species. *J. Biol. Chem.* 267(19): 13293-13301
- Chung, C. T., Nimrils, S.L., and Miller, R.H. 1989. One-step preparation of competent *Escherichia coli*. Transformation and storage of bacterial cells in the

same solution. *Proc. Natl. Acad. Sci. USA* 86, 2172-2175

Claiborne, A., and I. Fridovich. 1979. Purification of the o-dianisidine peroxidase from *Escherichia coli* B. Physicochemical characterization and analysis of its dual catalytic and peroxidatic activities. *J. Biol. Chem.* 254:4245-4252

Claiborne, A., D.P. Malinowski, and I. Fridovich. 1979. Purification and characterization of hydroperoxidase II of *Escherichia coli*. *J. Biol. Chem.* 254:11664-11668

Clayton, R.K. 1959. Purified catalase from *Rhodospseudomonas spheroides*. *Biochim. Biophys. Acta* 36:40-47

Cross, C.E., b. Halliwell, E.T. Borish, W.A. Pryor, B.N. Ames, R.L. Saul, J.M. Mccord and D. Harman. 1987. Oxygen radicals and human disease. *Ann. Intern. Med.* 107:526-545

Davies, K.J., M.E. Delsignore and S.W. Lin. 1987. Protein damage by oxygen radicals: II. Modification of amino acids. *J. Biol. Chem.* 262:9902-9907

Davies, M.J. 1991. Identification of a globin free radical in equine myoglobin treated with peroxides. *Biochim. Biophys. Acta* 1077, 86-90

Davies, M.J., and Puppo, A. 1992. Direct detection of a globin-derived radical in leghaemoglobin treated with peroxides. *Biochem. J.* 281:197-201

Desiseroth, A. and A.L. Dounce. 1970. Catalase: physical and chemical properties, mechanism of catalysis and physiological role. *Physiol. Rev.* 50:319-375

Dickerson R.E., H.B. Gray, M.Y. Darensbourg and D.J. Darensbourg. 1984. *Chemical Principles*, 4th edit., The Benjamin/cummings, California

Demple, B. 1991. Regulation of bacterial oxidative stress genes. *Annu. Rev. Genet.* 25:315-337

Demple, B., and S. Linn. 1982. 5,6-saturated thymine lesions in DNA: production by ultraviolet light of hydrogen peroxide. *Nucl. Acids Res.* 10:3781-3789

Dolphin, D., Forman, A., Borg, D.C., Fajer, B., and Felton, R.H. 1971. Compounds I of catalase and horseradish peroxidase: π -cation radicals. *Proceedings of the National Academy of Sciences, USA.* 68(3):614-618

Doyle M. P., R. A. Pickering, T. M. DeWeert, J.W. Hoekara and D. Peter. 1981. Kinetics and mechanism of the oxidation of human deoxyhemoglobin by nitrites. *J. Biol. Chem.* 256: 12393-12398.

Dunford, H.B. 1991. Horseradish peroxidase: structure and kinetic properties. In: *Peroxidases in Chemistry and Biology*, Everse, J. et al., eds. 28:121-131. Boca Raton, Fla.

Esaka M. and I.Asahi. 1982. Purification and properties of catalase from sweet potato root microbodies. *Plant Cell Physiol.* 23: 315-322

Espinosa-Urgel-M; Tormo-A. 1996. Sigma-s-Dependent promoters in *Escherichia coli* are located in DNA regions with intrinsic curvature. *Nucleic Acids Research* 21(16): 3667-3670

Fenton, H.H.H. 1894. Oxidation of tartaric acid in presence of iron. *J.Chem. Soc., Lon.* 65:899-910

Farr. S.B. and I.Kogoma. 1991. Oxidative stress responses in *Escherichia coli* and *Salmonella typhimurium*. *Microbiol. Rev.* 55:561-585

Filho, C.M., M.E. Hoffman and R.Meneghini. 1984. Cell killing and DNA damage by hydrogen peroxide are mediated by intracellular iron. *Biochem. J.* 218:273-275

Fita I. and M.G. Rossmann. 1985. The active center of catalase. *J. Mol. Biol.* 185:21-37

Fridovich, I. 1978. The biology of oxygen radicals. *Science.* 201:875-880

Fridovich, S.H. and N.E. Porter. 1981. Oxidation of arachidonic acid in micelles by superoxide and hydrogen peroxide. *J.Biol. Chem.* 256:260-265

Friend, S.H., March, K.L., Hanania, G.I.H., and Gurd, F.R. N. 1980. *Biochemistry* 19: 3039-3047

Gentry, D.R., Hernandez, V.J., Nguyen, L.H., Jensen, D.B., and Cashel, M. 1993. Synthesis of the stationary phase sigma factor σ^S is positively regulated by ppGpp. *J.Bacteriol.* 175:7982-7989

Gibso, J.F., Ingram, D.J.E., and Nicholl, P. 1958,. *Nature.* 181:1398-1399

Gorden, J., and Small, P.L.C. 1993. Acid resistance in enteric bacteria. *Infec. Immun.* 61:364-367

Gottstein A. 1893. Über die zerlegung des wasserstoffsperoxyds durch die zellen, mit bemerkungen über eine makroskopische reaction für bacterien. *Virchows Arch. Path. Anat.* 133:295-307

Gouet, P. 1993. Determination de la structure 3-D de la catalase de la bacterie

***Proteus mirabilis* par diffraction aux rayons X: structure avec et sans NADPH [PhD thesis]. Univeristy of Paris, XI Orsay, France**

Gouet, P., H.M. Jouve, and O.Dideberg. 1995. Crystal structure of *Proteus mirabilis* catalase with and without bound NADPH. *J. Mol. Biol.* 249:933-954

Haber, F., and J.Weiss. 1934. The catalytic decompositon of hydrogen peroxide by iron salts. *Proc. Roy. Soc. Ser. A* 147:332-351

Hillar, A.P., P. Nicholls. 1992. A mechanism for NADPH inhibition of catalase compound II formation. *FEBS Lett.* 314: 179-182

Halliwell B., D.A. Rowley and J.M.C. Gutteridge. 1983. Transition metal catalysis and oxygen radical reactions. In *Life Chemistry Reports Supplement 2 (Oxidative damage and related enzymes-EMBO weekshop, 1983)* 8-14

Halliwell B. and J.M.C. Gutteridge. 1989. Free Radicals in Biology and Medicine. 2nd ed. Oxford university Press., New York.

Hiratsu, K., H.Shinagawa., K. Makino. 1995. Mode of promoter recognition by the *Escherichia coli* RNA polymerase holoenzyme containing the sigma-s subunit: Identification of the recognition sequence of the *fic* promoter. *Mole. Microbiol.* 18:841-850

Herbert D. and J.Pinsent. 1948. Crystalline bacterial catalase. *Biochem. J.* 43:193-204

Igarashi, T., Kono, Y.,Tanaka, K. 1996. Molecular cloning of manganese catalase from *Lactobacillus plantarum*. *Journal of Biological Chemistry* 271(47): 29521-29524

Imlay K.A. and I.Fridoxich. 1991. DNA damage by hydrogen peroxide through the Fenton reaction in vivo and in vitro. *Science.* 240: 640-642

Ivancich A, Barynin VV, Zimmermann JL. 1995. Pulsed EPR studies of the binuclear Mn(III)Mn(IV) center in catalase from *Thermus thermophilus*. *Biochemistry* 34(20):6628-39

Jouve, H.M., J. Pelmont and J.Gaillard. 1986. Interaction between pyridine adenine dinucleotides and bovine liver catalase: A chromatographic and spectral study. *Arch. Biochem. Biophys.* 248: 71-79.

Jouve, H.M., F. Beaumont, I. Leger, J.Foray and J. Pelmont. 1989. Tightly bound NADPH in *Proteus mirabilis* PR catalase. *Biochem. Cell biol.* 67: 271-277

Khangulov, S. V., Goldfeld, M. G., Gerasimenko, V. V., Andreeva, N. E., Barynin, V. V., Grebenko, A. I. 1990. Effect of anions and redox state on the activity of manganese containing catalase from *Thermus thermophilus*. *Journal of Inorganic Biochemistry*. 40(4): 279-292

Kirkmann, H.N. and G.F. Gaetani. 1984. Catalase: a tetrameric enzyme with four tightly bound molecules of NADPH. *Proc. Natl. Acad. Sci. UAS*. 81: 4343-4348

Klots, M.G., G. R. Klassen, and P. C. Loewen. 1997. Phylogenetic relationships among prokaryotic and eukaryotic catalases. *Mol. Biol. Evol.* 14(9):951-958

Kono, Y., and Fridovich, I. 1983. Isolation and characterization of the pseudocatalase of *Lactobacillus plantarum*. *J. Biol. Chem.* 258:6015-6019

Kunkel T.A., J.D. Roberts and R.A. Zakour. 1987. Rapid and efficient site-specific mutagenesis without phenotypic selection. *Methods Enzymol.* 154: 367-382

Kusano, S., and Ishihama, A. 1997. Stimulatory effect of trshalose on formaitoon and activity of *Escherichia coli* RNA polymerase $E\sigma^S$ holoenzyme. *J.Bacteriol.* 179:3649-3654.

Lange, R., Fischer, D., and Hengge-Aronis, R. 1995. Identification of transcriptional start sites and the role of ppGpp in the expression of rpoS, the structural gene for the σ^S subunit of RNA polymerase in *Escherichia coli*. *J. Bacteriol.* 177: 4676-4680

Lange, R., and Hengge-Aronis, R., 1991. Identification of a central regulator of stationary-phase expression in *Escherichia coli*. *Molec. Microbiol.* 5:49-59

Lange, R., and Hengge-Aronis, R., 1994. The cellular concentration of the subunit of RNA polymerase in *Escherichia coli* is controlled at the levels of transcription, translation, and protein stability. *Genes Dev.* 8:1600-1612

Layne E. 1957. Spectrophotometric and turbidometric methods for measuring proteins. *Methods Enzymol.* 3: 447-454.

Levitz, S.M. and R.D. Diamond. 1984. Killing of *Aspergillus fumigatus* spores and *Candida albicans* yeast phase by the iron-hydrogen peroxide-halide system. *Infect. Immun.* 43:1100-1102

Lin, J., Merryweather, J., Vitello, L.B., Erman, J. E. 1999. Metmyoglobin/azide: the effect of heme-linked ionizations on the rate of complex formation. *Archives of biochemistry and biophysics.* 362(1): 148-158

Loew. O. 1901. Catalase, A new enzyme of general occurrence with special reference to the tobacco plant. *U.S. Dept. Agr. Rep.* #68:47

- Loewen P.C. 1984. Isolation of catalase-deficient *Escherichia coli* mutants and genetic mapping of *katE*, a locus that affects catalase activity. *J. Bacteriol.* 157: 622-626
- Loewen, P.C. 1997. Bacterial catalases. In: Oxidative stress and the molecular biology of antioxidant defenses. p: 273-308. Cold Spring Harbour Press
- Loewen, P.C., Switala, J. 1986. Purification and characterization of catalase HPII from *Escherichia coli* K12. *Biochem. Cell Biol.* 64:638-646
- Loewen, P.C., J. Switala, Ingemar von Ossowski, A. Hillar, A. Christie, B. Tattris, and P. Nicholls. 1993. Catalase HPII of *Escherichia coli* catalyzes the conversion of protoheme to cis-heme d. *Biochemistry.* 32(38): 10159-10164
- Loewen, P.C., B.L. Triggs. 1984. Genetic mapping of *katF*, a locus that with *katE* affects the synthesis of a second catalase species in *Escherichia coli*. *J. Bacteriol.* 160: 668-675
- MaCann, M.P., Fraley, C.D., and Matin, A. 1993. The putative σ factor KatF is regulated posttranscriptionally during carbon starvation. *J. Bacteriol.* 175:2143-2149
- Marcocci L., J.J. Maguire, M.T. Droy-Lefaix and L. Packer. 1994. The nitric oxide scavenging properties of Ginkgo biloba extract eGb 761. *Biochem. Biophys. Res. Commun.* 201:748-755.
- Marquis, R.E. and S.Y. Shin. 1994. Mineralization and responses of bacterial spores in heat and oxidative agents. *FEMS Microbiol. Rev.* 14:375-379
- Mead, J.F. 1976. Free radical mechanisms of lipid damage and consequences for cellular membranes. In *free radicals in biology*. 51-68. W.A. Pryor (ed), academic Press, New York
- Mead D.A., E.S. Skorupa, B. Kemper. 1985. Single-stranded DNA SP6 promoter plasmids for engineering mutant RNAs and proteins: synthesis of a 'stretched' preparathyroid hormone. *Nucleic Acids Res.* 13: 1103-1118
- Meier, A. E., Whittaker, M. M., Whittaker, J., W. 1996. PR polarization studies on Mn catalase from *Lactobacillus plantarum*. *Biochemistry* 35(1): 348-360
- Meir, E., and E. Yagil. 1985. Further characterization of the two catalases in *Escherichia coli*. *Curr. Microbiol.* 12:315-320
- Meir, E., and E. Yagil. 1990. Regulation of *Escherichia coli* catalases by anaerobiosis and catabolite repression. *Curr. Microbiol.* 20: 139-143

Melik-Adamyán, W.R., Barynin, V.V., Vagin, A. A. orisov, V.V., Vainshterin, B.K., Fita, I., Murthy, M.R.N., and Rossmann, M.G. 1986. Comparison of beef liver and *Penicillium vitale* catalases. *J. Molec. Biol.* 188:63-72

Miller, M.A., Bandyopadhyay, D., Mauro, J.M., Traylor, T.G., and Kraut, J. 1992. Reaction of ferrous cytochrome c peroxidase with dioxygen: Site-directed mutagenesis provides evidence for rapid reduction of dioxygen by intramolecular electron transfer from the compound I radical site. *Biochemistry.* 31:2789-2797

Muffler, a., Barth, M., Marschall, C., and Hengge-Aronis, R. 1997a. Heat shock regulation of σ^S turnover: a role for DnaK and relationship between stress responses mediated by σ^S and σ^{32} in *Escherichia coli*. *J. Bacteriol.* 179:445-452

Muffler, A., Fischer, D., Altuvia, S., Storz, G., and Hengge-Aronis, R. 1997c. The response regulator RssB controls stability of the σ^S subunit of RNA polymerase in *Escherichia coli*. *EMBO J.* 15:1333-1339

Muffler, A., Traulsen, D.D., Fischer, D., Lange, R., and Hengge-Aronis, R. 1997b. The RNA-binding protein HF-I plays a global regulatory role which is largely, but not exclusively, due to its role in expression of the subunit of RNA polymerase in *Escherichia coli*. *J. Bacteriol.* 179:297-300

Muffler A., Traulsen, D.D., Lange, R., and Hengge-Aronis, R. 1996. Posttranscriptional osmotic regulation of the σ^S subunit of RNA polymerase in *Escherichia coli*. *J. Bacteriol.* 178:1607-1613

Mulvey, M.R., Loewen, P.C. 1989. Nucleotide sequence of *katF* of *Escherichia coli* suggests *KatF* protein is a novel sigma transcription factor. *Nucleic Acids Res.* 17:9979-9991

Mulvey M.R., J. Switala, A. Borys, and P. C. Loewen. 1990. Regulation of Transcription of *katE* and *katF* in *Escherichia coli*. *J. Bacteriol.* 172:6713-6720

Murshodoc, G.N., A.I. Grebenko, V. Barynin, Z. Dauter, K.S. Wilson, B.K. Vainshtein, W. Melik-Adamyán, J. Bravo, J.M. Ferran, J.C. Ferrer, J. Switala, P.C. Loewen and I. Fita. 1996. Structure of the heme *d* of *Penicillium vitale* and *Escherichia coli* catalases. *J. Biol. Chem.* 271:8863-8868

Mulvey M.R., P.A. Sorby, B.L. Triggs-Raine and P.C. Loewen. 1988. Cloning and physical characterization of *katE* and *katF* required for catalase HP11 expression in *Escherichia coli*. *Gene* 73: 337-345.

Murshudov, G.N., W.R. Melik-Adamyán, A.I. Grebenko, V.V. Barynin, A.A. Vagin, B.K. Vainshterin, Z. Dauter, and K.S. Wilson. 1992. Three-dimensional structure of catalase from *Micrococcus lysodeikticus* at 1.5Å resolution. *FEBS Lett.* 312: 127-131.

- Murthy, M.R.N., T.J.Reid, A.Sicignano, N.tanaka and M.G. Rossmann. 1981. Structure of beef liver catalase. *J.Mol. Biol.* 152:465-499
- Nicholls, P. 1964. *Biochem. Biophys. Acta.* 81:479-495
- Nicholls, P. and G.R. Schonbaum. 1963. Catalases. In *The Enzymes*, Vol. 8,147-225, 2nd edit, P.D. Boyer, H.Lardy and K. Myrback (eds.), Academic Press, New York
- Obinger, C., m.Maj, P. Nichills, and P.Loewen, 1997. Activity, peroxide compound formation, and heme d synthesis in *Escherichia coli* HP11 catalase. *Arch. Biochem. Biophys.* 342(1):58-67
- Ortiz de Montellano, P.R. 1992. Catalytic sites of hemoprotein peroxidases. *Annual Review of Pharmacology and Toxicology.* 32:89-107
- Palaniappan, V. and Temer, J. 1990. Resonance Raman spectroscopic characterization of horseradish peroxidase intermediates. In: *Biological Oxidation systems.* Reddy, C.C.*et al.* edits. Vol.1:487-503. Academic Press., San Diego
- Pratt, L.A., and Silhavy, T.J. 1996. The response regulator SprE controls the stability of RpoS. *Proc. Natl. Acad.Sci. USA* 93:2488-2492
- Rorth M. and P.K. Jensen. 1967. Determination of catalase activity by means of the Clark electrode. *Biochim. Biophys. Acta.* 139:171-173
- Ruis,H., 1979. The biosynthesis of catalase. *Can. J. Biochem.* 57:1122-1130
- Sambrook J., E.F. Fritsch and T. Maniatis. 1989. *Molecular Cloning: A laboratory manual*, Cold Spring Harbor Laboratory, Cold Spring Harbor, New York
- Sanger, F.S., S. Nicklen and Coulson, A.R. 1977. DNA sequencing with chain-terminating inhibitors. *Proc. Natl. Acad.Sci. USA* 74:5463-5467.
- Schweder, T., Lee, K-. H., Lonovskaya, O., and Matin, A. 1996. Regulation of *Escherichia coli* starvation sigma factor (σ^S) by ClpXP protease. *J. Bacteriol.* 178:470-476
- Sevinc, M.S. 1997 Probing the structure and function of catalase HP11 of E.coli. (Ph.D. thesis)
- Sevinc, M.S., Switala, J., Bravo, J., I. Fita, and P.C. Loewen. 1998. Trunction and heme pocket mutations reduce production of functional catalase HP11 in *Escherichia coli*. *Pro. Eng.* 11(7):549-555

Sevinc, M.S., Werner Ens and P.C.Loewen, 1995. The cysteines of catalase HP11 of *Escherichia coli*, including Cys438 which is blocked, do not have a catalytic role. *Eur. j. biochem.* 230:127-132

Sevinc 1999 *Protein Science* 8:490-498

Shiba, T., Tsutsumi, K., Yano, H., Ihara, Y., Kameda, A., tanaka, K., takahashi, H., Munekata, M., Rao, N.N., and Kornberg, A. 1997. Inorganic polyphosphate and the induction of *rpoS* expression. *Proc. Natl. Acad. Sci. USA* 94:11210-11215

Sledjeski, D.D., Gupta, A., and Gottesman, S. 1996. The small RNA, Dsra, is essential for the low temperature expression of RpoS during exponential growth in *Escherichia coli*. *EMBO J.* 15:3993-4000

Small, P., Blankenhorn, D., Welty, D., Zinser, E., and Slonczewski, J.L. 1994. Acid and base resistance in *Escherichia coli* and *Shigella flexneri*: role of *rpoS* and growth pH. *J. Bacteriol.* 176: 1729-1737

Sumner, J.B. and A.I. Dounce. 1937. Crystallized catalase. *J.Biol. Chem.* 121:417-424

Switala, J., O'Neil, J., Loewen, P. C., 1999. Catalase HP11 from *Escherichia coli* exhibits enhanced resistance to denaturation. *Biochemistry.* 38: 3895-3901

Tanaka, K., Handel, K., Loewen, P.C., H.Takahashi. 1997. Identification and analysis of the *rpoS*-dependent promoter of *katE*, encoding catalase HP11 in *Escherichia coli*. *Bioch. Biophys. Acta.* 1352:161-166

Vieira J. and J.Messing. 1987. Production of single-stranded plasmid DNA. *Methods Enzymol.* 153:3-11

von Ossowski, I., Hausner, G., P.C. Loewen, 1993. Molecular evolutionary analysis based on the amino acid sequence of catalase. *J. Mol. Evol.* 37:71-76

von Ossowski I., MM.R. Mulvey, P.A. Leco, A. Borys, P.C.Loewen. 1991. Nucleotide sequence of *Escherichia coli katE*, which encodes catalase HP11. *J. Bacteriol.* 173:514-520

Weber K., J.T.Pringle & M. Osborn. 1972. Measurement of molecular weights by electrophoresis on SDS-acrylamide gels. *Methods Enzymol.* 26:3-27.

Xia Y, Roman LJ, Masters BS, Zweier JL. 1998. Inducible nitric-oxide synthase generates superoxide from the reductase domain. *J Biol Chem.* 273(35): 22635-22639

Yamashino, I., Ueguchi, C., and Mizuno, T. 1995. Quantitative control of the

stationary phase-specific sigma factor, σ^S , in *Escherichia coli*: involvement of the nucleoid protein H-NS. *EMBO J.* 14:594-602

Yanisch-Perron C., J. Vietra and J. Messing. 1985. Improved M13 phage cloning vectors and host strains: nucleotide sequence of the M13m18 and pUC19 vectors. *Gene* 33: 103-1194

Yusifov, E.F., A.I. Grebenko, V.V. Barynin, G.N. Murshundou, A.A. Vagin, W.R. Melik-Adamyanyan and B.K. Vainshtein. 1989. Three-dimensional structure of catalase from *Micrococcus lysodeikticus* at a resolution of 3.0 Å. *Sov. Phys. Crystallogr.* 34: 870-874

Zgurskaya, H.I., Keyhan, M., and Matin, A. 1997. The σ^S level in starving *Escherichia coli* cells increases solely as a result of its increased stability, despite decreased synthesis. *Molec. Microbiol.* 24: 643-651

Zhang, A., Altuvia, S., Tiwari, A., Hengge-Aronis, R., and Storz, G. 1998. The *oxyS* regulatory RNA represses *rpoS* translation by binding Hfq(HF-I). *EMBO J.* In review

Zhao, Y., Hoganson, C., Babcock, G.T., Marletta, M. A., 1998. Structural changes in the heme proximal pocket induced by nitric oxide binding to soluble guanylate cyclase. *Biochemistry* 37: 12458-12464